Available online at http://scik.org
Commun. Math. Biol. Neurosci. 2024, 2024:107
https://doi.org/10.28919/cmbn/8862
ISSN: 2052-2541

THE CONSEQUENCES OF POLLUTION ON THE PRODUCER-CONSUMER-PREDATOR FOOD CHAIN DYNAMICS WHEN THE PREDATOR HAS ACCESS TO EXTRA FOOD

MUSLIM SAAD JABBAR[1], RAID KAMEL NAJI[2,*]

Department of Mathematics, College of Science, University of Baghdad, Baghdad, Iraq

Abstract: It is known that pollution can have significant consequences on the dynamics of the producer-consumer-predator food chain, especially when predators have access to extra food sources due to the impact of pollution on environmental resources. Consequently, this paper proposes and investigates a novel mathematical model of the food chain that involves Producer-Consumer-Predator with extra food sources for a predator in a polluted environment. All the solution properties are discussed. The equilibrium points are determined along with their local stability conditions. Lyapunov functions are proposed to discuss the possibility of global stability. The concentrates at which the system undergoes persistence are found. Local bifurcation analysis is carried out to understand the influence of parameters on the dynamics of the system. A numerical simulation of the system is applied to confirm the analytic findings.

Keywords: additional food; antipredator; pollution; hunting cooperation; food chain.

2020 AMS Subject Classification: 92D25, 34L30, 92D40.

1. INTRODUCTION

One of the traditional uses of biological mathematics is to examine the interactions among species using differential equation models because predator-prey interactions have a strong effect on the dynamical system, where predators play an important role in preserving the food chain

---

*Corresponding author
E-mail address: raid.naji@sc.uobaghdad.edu.iq
Received August 23, 2024

structure. Furthermore, the most fundamental concept in predator-prey interaction is the functional response, which determines the rate at which a predator attacks a prey. There are several sorts of functional responses, including Holling type I, Holling type II, Holling type III, ratio-dependent, see [1-3] and the references therein, and Sokol-Howell [4], which is an upgraded variant of Holling type III [5-6].

More than two species can be included in the prey-predator paradigm. Numerous research has integrated diverse ecosystem types and taken into consideration a variety of predator-prey interactions, making the model more sophisticated and realistic [7-8]. In a population system, there are often two types of predators: generalists, or predators like lions and leopards, and specialists, or consumers, like wild bulls and zebras. Specialist predators only rely on specific types of food (producing species) for their survival and well-being, but generalist predators must ingest a variety of food sources and attack ferociously on their favorite prey [9]. Over the years, the examination of ecosystems where the predator and primary prey are provided with distinct food sources has been the subject of much research due to its potential implications. This area of study has become increasingly important to biologists, theoretical and experimental ecologists, and mathematicians [10-11]. It has been demonstrated that increased food intake, in particular, reduces predation pressure on prey by diverting the predator's attention from the target [12].

Cooperation in hunting, which is seen as the antithesis of self-interest, is one of the procedures that necessitate the availability of several species. This has reduced the amount of time and effort required for a hunt and increased hunting success rates [13]. There are predators in ecological systems that hunt in packs. This cooperative hunting often causes anxiety in the prey group; in such cases, the prey tends to flee or hide in a specific area [14-15]. Consequently, hunting cooperation increases fear indirectly.

One mechanism that reduces predation rates through evading or hiding from high-risk areas is assumed to be the prey's dread of becoming prey. Fear is an ecological component that rarely results in death, but it can stop prey from spreading since it makes it hide and reduces the likelihood that it will reproduce. The victim becomes afraid as a result of the predator's terror. On rare occasions, this effect may be about equal to the direct impact's magnitude [16-18]. Wang et al [14] presented a predator-prey model that takes into account the effect of anxiety on the growth of the prey. Similar to the predator-prey paradigm, fear could stabilize systems by preventing population fluctuations. The study discovered that, for particular parameter combinations, fear could have an impact on the stability of limit cycle oscillations. An effect not observed in conventional predator-prey models is the ability of fear to change population oscillation from supercritical to subcritical.

Antipredator behavior is now very common. Predator and prey have both evolved to adapt in ways that lead to this behavior. When prey displays antipredator behavior, it can protect itself from potential predators. The prey-predator model's dynamics, including antipredator behavior, have been the subject of several studies [19-20]. Their findings in the subsequent study [21] added to our understanding of the mechanisms underlying natural selection, particularly as they relate to the effects of antipredator behavior. The predator has an easier time surviving since it is less susceptible to antipredator measures. To illustrate antipredator behavior, they used the Holing type II function $f(x,y)=\frac{cxy}{1+my}$, where x is the prey, y is the predator, while m and c stand for two parameters that describe antipredator behavior.

Pollution of the environment is a significant influencing factor when dealing with natural resources. Pollution, exploitation, and interdependence may decrease stocks, reduce production, and lead to species extinction. Effective resource management, including pollution control, is crucial for the ecosystem's survival and production. Numerous studies show the impact of exploitation and pollution on the prey-predator system [22-25]. For instance, the study presented by Zawka and Srinivasu [26] deals with equations describing prey-predator interactions in the context of prey harvesting and reducing pollution activities. They conclude that Pollutants from outside sources affect the growth rates of both species, lowering the value of the resource.

Considering the aforementioned, despite the components' obvious presence in the condom, no research on an ecosystem has examined how the factors come together, which is the goal of this study. For example, some of these biological components have been included in certain earlier research. A mathematical model of the food chain focusing on the dynamics of prey, predator, and scavenger populations was proposed and examined by Satar and Naji [27]. In this model, toxicants have a direct impact on the growth of all prey, predator, and scavenging populations. According to the analysis, only external sources are responsible for the pollution releases. The dynamics and ideal harvesting of a prey-predator system in a polluted environment with scavengers and pollution control are the topics of Zawka and Melese [28]. They noticed that the environment is contaminated by toxicants that are emitted from outside sources and the dead corpses of predators and prey. This reduces the amount of money that can be made from harvesting because it hinders the growth of both predators and prey. A mathematical eco-epidemiological model comprising a prey-predator model with sickness in predators involving fear created owing to the intensity of hunting cooperation and anti-predator property was proposed and researched by Sahi and Satar [29]. Conversely, Hadi and Bahlool [30] looked at and suggested a nutritional chain model that included alternate food sources and a prey shelter. They hypothesized a positive correlation between the quantity of mid-predators and the number of refuges. A mathematical model that mimics the connection between prey and predator in the event of an infectious disease spreading throughout the predator population and the creation of new food sources for the predator has recently been developed and studied in [31]. Presumably, the prey slows down its growth rate because it feels compelled by the predator's wrath to find a place where it will feel secure and afraid.

Consequently, in this paper, a mathematical model of the food chain consisting of producer-consumer-predator that involves fear, hunting cooperation, antipredator, and additional food has been proposed and formulated mathematically in the next section. The equilibria's existence and local stability were discussed in section 3. Section 4 treats the determination of persistence requirements. The global stability analysis was the subject of section 5. Section 6, determines the local bifurcation of the system. A numerical simulation was applied to understand the system's dynamics in section 7. Finally, Section 8 summarizes the conclusions of the study.

2. THE MODEL FORMULATION

This section formulates an ecological food chain model that considers fear, hunting cooperation, antipredator, and additional food. Throughout the formulation process the following assumptions are adopted:

In the absence of the consumer, the producer grows logistically, whereas in the presence of the consumer, it decays due to feed-on employing a linear functional response. Fear is often induced in the consumer when predators hunt together. This disrupts the consumer's feeding patterns and limits the amount of food obtained from the producer. The Sokol and Howell functional response will be appropriate for the predation mechanism since consumers are capable of cooperative defense and possibly killing the predator. Also, due to the availability of additional food for the predator, represented by the term $\alpha\beta A$, a decrease in the rate of predation for the consumer will be observed. Moreover, the system is being operated in a polluted environment. External pollutants, such as industrial waste, can affect the populations of both consumer and predator species. As a result, the dynamics of such a system can be quantitatively simulated using the following first-order differential equations:

$$\begin{aligned}
\frac{dX}{dT} &= rX\left(1-\frac{X}{k}\right)-\frac{a_0XY}{1+nZ} = Xf_1(X,Y,Z),\\
\frac{dY}{dT} &= \frac{a_1XY}{1+nZ}-\frac{(a_2+cZ)YZ}{1+\alpha\beta A+m_0Y^2}-q_1Y^3-d_0Y = Yf_2(X,Y,Z),\\
\frac{dZ}{dT} &= \frac{e(a_2+cZ)(Y+\beta A)Z}{1+\alpha\beta A+m_0Y^2}-\frac{q_0YZ}{1+m_1Z}-q_2Z^2-d_1Z = Zf_3(X,Y,Z),
\end{aligned} \tag{1}$$

where $X(0) \geq 0$, $Y(0) \geq 0$, and $Z(0) \geq 0$. Table 1 lists the variables and positive parameter descriptions.

Table 1: Description of model variables and parameters:

Symbols	Description
$\boldsymbol{X(T)}$	The density of producer population at time $\boldsymbol{T}$.
$\boldsymbol{Y(T)}$	The density of consumer population at time $\boldsymbol{T}$.
$\boldsymbol{Z(T)}$	The density of predator population at time $\boldsymbol{T}$.
$\boldsymbol{r}$	Intrinsic growth rate for the producer.
$\boldsymbol{k}$	Carrying capacity of the producer.
$\boldsymbol{a_0}$	The consumer attack rate against producers.
$\boldsymbol{a_1 = e_0a_0}$	The rate at which the producer's biomass is converted to the consumer's biomass such that $\boldsymbol{e_0 \in (0,1)}$.
$\boldsymbol{a_2}$	The predator's attack rate against consumers.
$\boldsymbol{m_0}$	Handling time constant.
$\boldsymbol{c}$	The level of cooperation between predators when hunting.
$\boldsymbol{n}$	Consumers' level of fear of predators.
$\boldsymbol{q_0}$	The level of antipredator in the consumer.
$\boldsymbol{m_1}$	Predator efficiency to avoid the anti-predator capability in the consumer
$\boldsymbol{d_0, d_1}$	Natural death rates for the consumer and the predator, respectively.
$\boldsymbol{e \in (0,1)}$	The rate at which the consumer's biomass is converted to the predator's biomass.
$\boldsymbol{q_1}$	Toxicity coefficient for consumers.
$\boldsymbol{q_2}$	Toxicity coefficient for predators.
$\boldsymbol{\alpha}$	The quality of additional food.
$\boldsymbol{\beta A}$	The effective additional food-level term.

To simplify the system (1), the dimensionless parameters and variables mentioned below will be utilized:

$$x = \frac{X}{k}, y = \frac{a_0 Y}{r}, z = nZ, t = rT,$$
$$\mu_1 = \frac{a_1 k}{r}, \mu_2 = \frac{a_2}{rn}, \mu_3 = \frac{c}{na_2}, \mu_4 = \alpha\beta A, \mu_5 = \frac{m_0 r^2}{a_0^2}, \mu_6 = \frac{q_1 r}{a_0^2},$$
$$\mu_7 = \frac{d_0}{r}, \mu_8 = \frac{e a_2}{a_0}, \mu_9 = \frac{q_0}{a_0}, \mu_{10} = \frac{m_1}{n}, \mu_{11} = \frac{q_2}{nr}, \mu_{12} = \frac{d_1}{r}, \mu_{13} = \frac{\beta A a_0}{r}.$$

The dimensionless system can be expressed as follows:

$$\begin{aligned} \frac{dx}{dt} &= x\left(1 - x - \frac{y}{1+z}\right) = x f_1(x,y,z), \\ \frac{dy}{dt} &= y\left(\frac{\mu_1 x}{1+z} - \frac{\mu_2(1+\mu_3 z)z}{1+\mu_4+\mu_5 y^2} - \mu_6 y^2 - \mu_7\right) = y f_2(x,y,z), \\ \frac{dz}{dt} &= z\left(\frac{\mu_8(1+\mu_3 z)(y+\mu_{13})}{1+\mu_4+\mu_5 y^2} - \frac{\mu_9 y}{1+\mu_{10} z} - \mu_{11} z - \mu_{12}\right) = z f_3(x,y,z). \end{aligned} \tag{2}$$

The interaction functions of the system (2) are defined on $\mathbb{R}_+^3 = \{(x,y,z): x(0) \geq 0, y(0) \geq 0, z(0) \geq 0\}$. The functions f_1, f_2, and f_3 on the right-hand side of the system (2) have continuous partial derivatives and thus are said to be continuous. Therefore, these functions satisfy Lipschitz's criterion. Given the initial conditions $x(0) \geq 0, y(0) \geq 0$, and $z(0) \geq 0$, the solution exists and is unique, according to the fundamental theorem of existence and uniqueness.

Theorem 1. For all $t \geq 0$, System (2) is positively invariant for all positive initial values.

Proof. Define $\Omega = \{(x,y,z) \in \mathbb{R}_+^3 : x > 0, y > 0, z > 0\}$. Applying the initial conditions $x(0) > 0$, $y(0) > 0$, and $z(0) > 0$ to the mathematical equations of system (2) yields the following result:

$$x(t) = x(0) e^{\int_0^t \left[1 - x(s) - \frac{y(s)}{1+z(s)}\right] ds}$$

$$y(t) = y(0) e^{\int_0^t \left[\frac{\mu_1 x(s)}{1+z(s)} - \frac{\mu_2(1+\mu_3 z(s))z(s)}{1+\mu_4+\mu_5 (y(s))^2} - \mu_6 (y(s))^2 - \mu_7\right] ds}$$

$$z(t) = z(0) e^{\int_0^t \left[\frac{\mu_8(1+\mu_3 z(s))(y(s)+\mu_{13})}{1+\mu_4+\mu_5 (y(s))^2} - \frac{\mu_9 y(s)}{1+\mu_{10} z(s)} - \mu_{11} z(s) - \mu_{12}\right] ds}$$

The exponential function defines that all solutions in Ω with positive initial conditions remain in the first octant. Hence, the proof is done. ■

In theoretical ecology, the system's boundedness indicates that it is biologically well-behaved. Because the solutions are bounded, none of the species that interact will grow fast or exponentially over time, due to a shortage of supplies, any species' population is limited.

Theorem 2. In the region,

$$\Psi = \left\{(x,y,z) \in \mathbb{R}^3_+ : 0 < x(t) < 1, 0 < x(t) + \frac{1}{\mu_1}y(t) + \frac{\mu_2}{\mu_1\mu_8}z(t) \leq \frac{2}{\beta}\right\}.$$

All solutions of the system (2), which initiates in $\mathbb{R}^3_+$ are uniformly bounded if the following sufficient condition is met.

$$\mu_8\mu_{13} < \min\left\{\mu_{12}(1+\mu_4), \frac{\mu_{11}(1+\mu_4)}{\mu_3}\right\}. \tag{3}$$

Proof. Consider the solution $(x(t), y(t), z(t))$ of the system (2). Then the first equation in system (2) indicates that $\frac{dx}{dt} \leq x - x^2$. By using lemma (2.2) [32], this inequality's solution is provided by $x(t) \leq \frac{x_0}{e^{-t}(1-x_0)-x_0}$, where x_0 is the initial value s.t. $x_0 = x(0)$. As t approaches ∞, the solution $x(t)$ ensures that $x \leq 1$.

Now, define the function $H(t) = x(t) + \frac{1}{\mu_1}y(t) + \frac{\mu_2}{\mu_1\mu_8}z(t)$. Differentiating $H(t)$ gives:

$$\begin{aligned}\frac{dH}{dt} &= x(1-x) - \frac{xy}{1+z} + \frac{1}{\mu_1}\left(\frac{\mu_1 xy}{1+z} - \frac{\mu_2(1+\mu_3 z)yz}{1+\mu_4+\mu_5 y^2} - \mu_6 y^3 - \mu_7 y\right) \\ &+ \frac{\mu_2}{\mu_1\mu_8}\left(\frac{\mu_8(1+\mu_3 z)(y+\mu_{13})z}{1+\mu_4+\mu_5 y^2} - \frac{\mu_9 yz}{1+\mu_{10}z} - \mu_{11}z^2 - \mu_{12}z\right).\end{aligned}$$

Direct computation leads to:

$$\frac{dH}{dt} \leq x - \frac{1}{\mu_1}\mu_7 y - \frac{\mu_2}{\mu_1\mu_8}\left[\mu_{12} - \frac{\mu_8\mu_{13}}{1+\mu_4}\right]z - \frac{\mu_2}{\mu_1}\left[\frac{\mu_{11}}{\mu_8} - \frac{\mu_3\mu_{13}}{1+\mu_4}\right]z^2.$$

Furthermore, using the sufficient condition it is obtained that

$$\frac{dH}{dt} \leq 2 - \beta H,$$

where $\beta = \min\left\{1, \mu_7, \mu_{12} - \frac{\mu_8\mu_{13}}{1+\mu_4}\right\}$.

Using lemma (2.1) [32], it is found that $H(t) \leq \frac{2}{\beta}$ as t approaches ∞. Thus, the solutions of system (2) in the region Ψ are uniformly bounded with the initial point being non-negative. Hence, the proof is done. ■

It is commonly understood that an ecological system is dissipative if the environment equally limits each population. Consequently, system (2) has dissipative properties.

3. Existence and Local Stability of Equilibrium Points

The presence of non-negative equilibria is examined, and the stability requirements around these equilibria are established. The non-negative equilibrium points are defined as follows:

- The trivial point denoted by $e_0 = (0,0,0)$ is always exists.
- The first axial point denoted by $e_1 = (1,0,0)$ is always exists.
- The second axial point denoted by $e_2 = (0,0,\tilde{z})$, where $\tilde{z} = \frac{\mu_8\mu_{13}-(1+\mu_4)\mu_{12}}{(1+\mu_4)\mu_{11}-\mu_3\mu_8\mu_{13}}$, which exists provided that one of the following conditions holds:

$$\left.\begin{array}{c} (1+\mu_4)\mu_{12} < \mu_8\mu_{13} < \frac{(1+\mu_4)\mu_{11}}{\mu_3} \\ or \\ \frac{(1+\mu_4)\mu_{11}}{\mu_3} < \mu_8\mu_{13} < (1+\mu_4)\mu_{12} \end{array}\right\} . \qquad (4)$$

- The first planar point denoted by $e_3 = (1,0,\tilde{z})$ which is exists under the condition (4) too.
- The second planar point $e_4 = (\hat{x},\hat{y},0)$, where $\hat{x} = 1-\hat{y}$, while $\hat{y}$ is a positive root of the second-order polynomial $-\mu_6 y^2 - \mu_1 y + \mu_1 - \mu_7 = 0$. This polynomial has a unique positive root written by $\hat{y} = -\frac{\mu_1}{2\mu_6} + \frac{\sqrt{\mu_1{}^2+4\mu_6(\mu_1-\mu_7)}}{2\mu_6}$, provided that:

$$\mu_7 < \mu_1. \qquad (5)$$

Accordingly, the point e_4 will exist uniquely when a positive root $\hat{y}$ satisfies:

$$\hat{y} < 1. \qquad (6)$$

- The positive point denoted by $e_5 = (\bar{x},\bar{y},\bar{z})$, where $\bar{x} = \frac{1-\bar{y}+\bar{z}}{1+\bar{z}}$ while the $(\bar{y},\bar{z})$ is the positive intersection point of the isoclines:

$$\begin{array}{l} h_1(y,z) = \frac{(1-y+z)\mu_1}{1+z} - z\mu_2 - z^2\mu_2 - z^2\mu_2\mu_3 - z^3\mu_2\mu_3 + \frac{(1-y+z)\mu_1\mu_4}{1+z} \\ \quad + \frac{y^2(1-y+z)\mu_1\mu_5}{1+z} - y^2\mu_6 - y^2 z\mu_6 - y^2\mu_4\mu_6 - y^2 z\mu_4\mu_6 - y^4\mu_5\mu_6 \\ \quad -y^4 z\mu_5\mu_6 - \mu_7 - z\mu_7 - \mu_4\mu_7 - z\mu_4\mu_7 - y^2\mu_5\mu_7 - y^2 z\mu_5\mu_7 = 0. \end{array}$$

$$\begin{array}{l} h_2(y,z) = -y\mu_8 - yz\mu_3\mu_8 + y\mu_9 + y\mu_4\mu_9 + y^3\mu_5\mu_9 - yz\mu_8\mu_{10} \\ \quad -yz^2\mu_3\mu_8\mu_{10} + z\mu_{11} + z\mu_4\mu_{11} + y^2 z\mu_5\mu_{11} + z^2\mu_{10}\mu_{11} + z^2\mu_4\mu_{10}\mu_{11} \\ \quad +y^2 z^2\mu_5\mu_{10}\mu_{11} + \mu_{12} + \mu_4\mu_{12} + y^2\mu_5\mu_{12} + z\mu_{10}\mu_{12} + z\mu_4\mu_{10}\mu_{12} \\ \quad +y^2 z\mu_5\mu_{10}\mu_{12} - \mu_8\mu_{13} - z\mu_3\mu_8\mu_{13} - z\mu_8\mu_{10}\mu_{13} - z^2\mu_3\mu_8\mu_{10}\mu_{13} = 0. \end{array}$$

It is easy to verify that as $z \to 0$ the above two isoclines become

$$\begin{array}{l} h_1(y,0) = -\mu_5\mu_6 y^4 - \mu_1\mu_5 y^3 + (\mu_1\mu_5 - \mu_6 - \mu_4\mu_6 - \mu_5\mu_7)y^2 \\ \qquad -(\mu_1 + \mu_1\mu_4)y + \mu_1 + \mu_1\mu_4 - \mu_7 - \mu_4\mu_7 = 0 \end{array} .$$

$$\begin{array}{l} h_2(y,0) = \mu_5\mu_9 y^3 + \mu_5\mu_{12} y^2 + (-\mu_8 + \mu_9 + \mu_4\mu_9)y \\ \qquad +\mu_{12} + \mu_4\mu_{12} - \mu_8\mu_{13} = 0 \end{array} .$$

Direct computation shows that the first isocline has a unique positive root for y denoted by y_1 if the following condition holds

$$\mu_7 < \mu_1 < \frac{\mu_6(1+\mu_4)}{\mu_5} + \mu_7. \tag{7}$$

While the second isocline has a unique positive root for y denoted by y_2 if the following condition holds

$$\mu_{12}(1+\mu_4) < \mu_8\mu_{13}. \tag{8}$$

Consequently, the above two isoclines have a unique intersection positive point denoted by $(\bar{y},\bar{z})$ if the following sufficient conditions hold:

$$\left.\begin{array}{l} y_1 < y_2 \\ \frac{dz}{dy} = -\frac{(\partial h_1/\partial y)}{(\partial h_1/\partial z)} > 0 \\ \frac{dz}{dy} = -\frac{(\partial h_2/\partial y)}{(\partial h_2/\partial z)} < 0 \end{array}\right\}. \tag{9}$$

Finally, the positive equilibrium point exists uniquely if the following condition is met in addition to the above set of sufficient conditions.

$$\bar{y} < 1 + \bar{z}. \tag{10}$$

In the next steps, the linearization technique is used to analyze the system's local stability around the previously discussed equilibrium points. Now the basic Jacobian matrix of system (2) is determined as follows:

$$J(x,y,z) = \begin{pmatrix} x\frac{\partial f_1}{\partial x} + f_1 & x\frac{\partial f_1}{\partial y} & x\frac{\partial f_1}{\partial z} \\ y\frac{\partial f_2}{\partial x} & y\frac{\partial f_2}{\partial y} + f_2 & y\frac{\partial f_2}{\partial z} \\ z\frac{\partial f_3}{\partial x} & z\frac{\partial f_3}{\partial y} & z\frac{\partial f_3}{\partial z} + f_3 \end{pmatrix} = \left(a_{ij}\right)_{3\times 3}, \tag{11}$$

where:

$$a_{11} = -x + \left[1 - x - \frac{y}{1+z}\right],\ a_{12} = -\frac{x}{1+z},\ a_{13} = \frac{xy}{(1+z)^2},$$

$$a_{21} = \frac{\mu_1 y}{1+z},\ a_{22} = \frac{2\mu_2\mu_5(1+\mu_3 z)y^2 z}{(1+\mu_4+\mu_5 y^2)^2} - 2\mu_6 y^2 + \left[\frac{\mu_1 x}{1+z} - \frac{\mu_2(1+\mu_3 z)z}{1+\mu_4+\mu_5 y^2} - \mu_6 y^2 - \mu_7\right],$$

$$a_{23} = -\left(\frac{\mu_1 x}{(1+z)^2} + \frac{\mu_2(1+2\mu_3 z)}{1+\mu_4+\mu_5 y^2}\right)y,\ a_{31} = 0,$$

$$a_{32} = \left(\frac{\mu_8(1+\mu_3 z)}{1+\mu_4+\mu_5 y^2} - \frac{\mu_9}{1+\mu_{10} z} - \frac{2\mu_5\mu_8(1+\mu_3 z)(y+\mu_{13})y}{(1+\mu_4+\mu_5 y^2)^2}\right)z,$$

$$a_{33} = \frac{\mu_3\mu_8(y+\mu_{13})z}{1+\mu_4+\mu_5 y^2} + \frac{\mu_9\mu_{10} yz}{(1+\mu_{10} z)^2} - \mu_{11} z + \left[\frac{\mu_8(1+\mu_3 z)(y+\mu_{13})}{1+\mu_4+\mu_5 y^2} - \frac{\mu_9 y}{1+\mu_{10} z} - \mu_{11} z - \mu_{12}\right].$$

So, at the trivial point e_0, matrix (11) yields:

$$J(e_0) = \begin{pmatrix} 1 & 0 & 0 \\ 0 & -\mu_7 & 0 \\ 0 & 0 & \frac{\mu_8\mu_{13}}{1+\mu_4} - \mu_{12} \end{pmatrix}. \tag{12}$$

Thus, $J(e_0)$ has the following eigenvalues: $\lambda_{01}=1$, $\lambda_{02}=-\mu_7$, and $\lambda_{03}=\frac{\mu_8\mu_{13}}{1+\mu_4}-\mu_{12}$. Therefore, e_0 is a saddle point.

Also, at the first axial point e_1, matrix (11) yields:

$$J(e_1)=\begin{pmatrix}-1 & -1 & 0\\ 0 & \mu_1-\mu_7 & 0\\ 0 & 0 & \frac{\mu_8\mu_{13}}{1+\mu_4}-\mu_{12}\end{pmatrix} \tag{13}$$

The eigenvalues of $J(e_1)$ are $\lambda_{11}=-1$, $\lambda_{12}=\mu_1-\mu_7$, and $\lambda_{13}=\frac{\mu_8\mu_{13}}{1+\mu_4}-\mu_{12}$. Therefore, e_1 is locally asymptotically stable, assuming that the following conditions hold:

$$\mu_1<\mu_7. \tag{14}$$

$$\mu_8\mu_{13}<\mu_{12}(1+\mu_4). \tag{15}$$

At the second axial point e_2, matrix (11) yields:

$$J(e_2)=\begin{pmatrix}1 & 0 & 0\\ 0 & -\frac{\mu_2(1+\mu_3\tilde{z})\tilde{z}}{1+\mu_4}-\mu_7 & 0\\ 0 & \left(\frac{\mu_8(1+\mu_3\tilde{z})}{1+\mu_4}-\frac{\mu_9}{1+\mu_{10}\tilde{z}}\right)\tilde{z} & \left(\frac{\mu_3\mu_8\mu_{13}}{1+\mu_4}-\mu_{11}\right)\tilde{z}\end{pmatrix}. \tag{16}$$

Thus, $J(e_2)$ has the following eigenvalues: $\lambda_{21}=1$, $\lambda_{22}=-\frac{\mu_2(1+\mu_3\tilde{z})\tilde{z}}{1+\mu_4}-\mu_7$, and $\lambda_{23}=\left(\frac{\mu_3\mu_8\mu_{13}}{1+\mu_4}-\mu_{11}\right)\tilde{z}$. Therefore, e_2 is a saddle point.

At the first planar point e_3, matrix (11) yields:

$$J(e_3)=\begin{pmatrix}-1 & -\frac{1}{1+\tilde{z}} & 0\\ 0 & \frac{\mu_1}{1+\tilde{z}}-\frac{\mu_2(1+\mu_3\tilde{z})\tilde{z}}{1+\mu_4}-\mu_7 & 0\\ 0 & \left(\frac{\mu_8(1+\mu_3\tilde{z})}{1+\mu_4}-\frac{\mu_9}{1+\mu_{10}\tilde{z}}\right)\tilde{z} & \left(\frac{\mu_3\mu_8\mu_{13}}{1+\mu_4}-\mu_{11}\right)\tilde{z}\end{pmatrix}. \tag{17}$$

Thus, $J(e_3)$ has the following eigenvalues: $\lambda_{31}=-1$, $\lambda_{32}=\frac{\mu_1}{1+\tilde{z}}-\frac{\mu_2(1+\mu_3\tilde{z})\tilde{z}}{1+\mu_4}-\mu_7$, and $\lambda_{33}=\left(\frac{\mu_3\mu_8\mu_{13}}{1+\mu_4}-\mu_{11}\right)\tilde{z}$. Therefore, e_3 is locally asymptotically stable, assuming that the following conditions hold:

$$\frac{\mu_1}{1+\tilde{z}}<\frac{\mu_2(1+\mu_3\tilde{z})\tilde{z}}{1+\mu_4}+\mu_7. \tag{18}$$

$$\mu_8\mu_{13}<\frac{\mu_{11}(1+\mu_4)}{\mu_3}. \tag{19}$$

Moreover, at the second planar point, the matrix (11) yields:

$$J(e_4) = \begin{pmatrix} -\hat{x} & -\hat{x} & \hat{x}\hat{y} \\ \mu_1\hat{y} & -2\mu_6\hat{y}^2 & -\mu_1\hat{x}\hat{y} - \frac{\mu_2\hat{y}}{1+\mu_4+\mu_5\hat{y}^2} \\ 0 & 0 & \frac{\mu_8(\hat{y}+\mu_{13})}{1+\mu_4+\mu_5\hat{y}^2} - \mu_9\hat{y} - \mu_{12} \end{pmatrix} = (\hat{a}_{ij}). \quad (20)$$

The eigenvalues of $J(e_4)$ are $\lambda_{41,42} = \frac{\hat{a}_{11}+\hat{a}_{22}}{2} \pm \frac{\sqrt{(\hat{a}_{11}+\hat{a}_{22})^2 - 4(\hat{a}_{11}\hat{a}_{22} - \hat{a}_{12}\hat{a}_{21})}}{2}$, and $\lambda_{43} = \hat{a}_{33}$. Since $\hat{a}_{11}\hat{a}_{22} - \hat{a}_{12}\hat{a}_{21} = 2\mu_6\hat{x}\hat{y}^2 + \mu_1\hat{x}\hat{y} > 0$, and $\hat{a}_{11} + \hat{a}_{22} < 0$, hence λ_{41} and λ_{42} are negative real parts eigenvalues. Thus, e_4 is locally asymptotically stable, provided the following condition holds:

$$\frac{\mu_8(\hat{y}+\mu_{13})}{1+\mu_4+\mu_5\hat{y}^2} < \mu_9\hat{y} + \mu_{12}. \quad (21)$$

Additionally, the matrix (11) at the positive point e_5 is as follows:

$$J(e_5) = \begin{pmatrix} \bar{a}_{11} & \bar{a}_{12} & \bar{a}_{13} \\ \bar{a}_{21} & \bar{a}_{22} & \bar{a}_{23} \\ 0 & \bar{a}_{32} & \bar{a}_{33} \end{pmatrix} \quad (22)$$

where:

$$\bar{a}_{11} = -\bar{x},\ \bar{a}_{12} = -\frac{\bar{x}}{1+\bar{z}},\ \bar{a}_{13} = \frac{\bar{x}\bar{y}}{(1+\bar{z})^2},\ \bar{a}_{21} = \frac{\mu_1\bar{y}}{1+\bar{z}},\ \bar{a}_{22} = \frac{2\mu_2\mu_5(1+\mu_3\bar{z})\bar{y}^2\bar{z}}{(1+\mu_4+\mu_5\bar{y}^2)^2} - 2\mu_6\bar{y}^2,$$

$$\bar{a}_{23} = -\bar{y}\left(\frac{\mu_1\bar{x}}{(1+\bar{z})^2} + \frac{\mu_2(1+2\mu_3\bar{z})}{1+\mu_4+\mu_5\bar{y}^2}\right),$$

$$\bar{a}_{32} = \bar{z}\left(\frac{\mu_8(1+\mu_3\bar{z})}{1+\mu_4+\mu_5\bar{y}^2} - \frac{2\mu_5\mu_8(1+\mu_3\bar{z})(\bar{y}+\mu_{13})\bar{y}}{(1+\mu_4+\mu_5\bar{y}^2)^2} - \frac{\mu_9}{1+\mu_{10}\bar{z}}\right),$$

$$\bar{a}_{33} = \frac{\mu_3\mu_8(\bar{y}+\mu_{13})\bar{z}}{1+\mu_4+\mu_5\bar{y}^2} + \frac{\mu_9\mu_{10}\bar{y}\bar{z}}{(1+\mu_{10}\bar{z})^2} - \mu_{11}\bar{z}.$$

As a result, the characteristic equation of $J(e_5)$ can be expressed as follows:

$$\lambda_3{}^3 + \alpha_1\lambda_3{}^2 + \alpha_2\lambda_3 + \alpha_3 = 0, \quad (23)$$

where:

$$\alpha_1 = -(\bar{a}_{11} + \bar{a}_{22} + \bar{a}_{33}),$$

$$\alpha_2 = \bar{a}_{11}\bar{a}_{22} + \bar{a}_{11}\bar{a}_{33} + \bar{a}_{22}\bar{a}_{33} - \bar{a}_{12}\bar{a}_{21} - \bar{a}_{23}\bar{a}_{32},$$

$$\alpha_3 = -\bar{a}_{33}(\bar{a}_{11}\bar{a}_{22} - \bar{a}_{12}\bar{a}_{21}) + \bar{a}_{32}(\bar{a}_{11}\bar{a}_{23} - \bar{a}_{21}\bar{a}_{13}),$$

with

$$\alpha_1\alpha_2 - \alpha_3 = -(\bar{a}_{11} + \bar{a}_{22})[\bar{a}_{11}\bar{a}_{22} - \bar{a}_{12}\bar{a}_{21}] - (\bar{a}_{22} + \bar{a}_{33})[\bar{a}_{22}\bar{a}_{33} - \bar{a}_{23}\bar{a}_{32}]$$
$$-\bar{a}_{11}\bar{a}_{33}(\bar{a}_{11} + 2\bar{a}_{22} + \bar{a}_{33}) + \bar{a}_{13}\bar{a}_{21}\bar{a}_{32}.$$

According to the Routh-Hurwitz criterion, $e_5 = (\bar{x}, \bar{y}, \bar{z})$ is locally asymptotically stable provided $\alpha_1 > 0, \alpha_3 > 0$ and $\alpha_1\alpha_2 > \alpha_3$, which is true if and only if the following conditions are satisfied:

$$\frac{\mu_3\mu_8(\bar{y}+\mu_{13})}{1+\mu_4+\mu_5\bar{y}^2}+\frac{\mu_9\mu_{10}\bar{y}}{(1+\mu_{10}\bar{z})^2}<\mu_{11}, \tag{24}$$

$$\frac{\mu_2\mu_5(1+\mu_3\bar{z})\bar{z}}{(1+\mu_4+\mu_5\bar{y}^2)^2}<\mu_6, \tag{25}$$

$$\frac{2\mu_5\mu_8(1+\mu_3\bar{z})(\bar{y}+\mu_{13})\bar{y}}{(1+\mu_4+\mu_5\bar{y}^2)^2}+\frac{\mu_9}{1+\mu_{10}\bar{z}}<\frac{\mu_8(1+\mu_3\bar{z})}{1+\mu_4+\mu_5\bar{y}^2}, \tag{26}$$

$$\frac{\mu_1\bar{y}}{(1+\bar{z})^3}<\frac{\mu_2(1+2\mu_3\bar{z})}{1+\mu_4+\mu_5\bar{y}^2}+\frac{\mu_1\bar{x}}{(1+\bar{z})^2}\ . \tag{27}$$

Consequently, the next theorem is verified.

Theorem 3. In system (2), the positive point is locally asymptotically stable if the conditions (24-27) are met.

4. PERSISTENCE

A system is said to be persistent if and only if all species survive. Mathematically, this means that with a positive initial condition of the system (2), if the solution does not have an omega limit set placed at the boundary of its domain, the system is said to persist.

The following expressions can be used to represent the possible subsystems located in the positive quadrant of the xz-plane and xy-plane of the system (2) respectively:

$$\begin{aligned}\frac{dx}{dt}&=x(1-x)=\beta_1(x,z),\\ \frac{dz}{dt}&=z\left(\frac{\mu_8(1+\mu_3 z)\mu_{13}}{1+\mu_4}-\mu_{11}z-\mu_{12}\right)=\beta_2(x,z).\end{aligned} \tag{28}$$

And

$$\begin{aligned}\frac{dx}{dt}&=x[1-x-y]=\beta_3(x,y),\\ \frac{dy}{dt}&=y[\mu_1 x-\mu_6 y^2-\mu_7]=\beta_4(x,y).\end{aligned} \tag{29}$$

The subsystems (28)-(29) in $\mathbb{R}^2_+$ have a positive equilibrium point that corresponds to $e_3=(1,0,\tilde{z})$ and $e_4=(\hat{x},\hat{y},0)$ of the system (2) respectively. To verify whether periodic dynamics exist near the interior positive point of the subsystems (28)-(29), the Dulac function approach [33] is used.

Let $g_1(x,z)=\frac{1}{xz,}$ and $g_2(x,y)=\frac{1}{xy}$ are continuously differentiable functions that are defined for every $(x,z),(x,y)\in\mathbb{R}^2_+$ and are located in the interior of the positive quadrant of the xz-plane and xy-plane, and $g_1(x,z)>0$ and $g_2(x,y)>0$. Furthermore, the straightforward calculation yields that:

$$\Delta_1(x,z)=\frac{\partial}{\partial x}(g_1.\beta_1)+\frac{\partial}{\partial z}(g_1.\beta_2)=-\frac{1}{z}-\frac{1}{x}\left(\mu_{11}-\frac{\mu_3\mu_8\mu_{13}}{(1+\mu_4)}\right).$$

$$\Delta_2(x,y)=\frac{\partial}{\partial x}(g_2.\beta_3)+\frac{\partial}{\partial y}(g_2.\beta_4)=-\frac{1}{y}-\frac{2\mu_6 y}{x}.$$

Then $\Delta_1(x,z)<0$ due to the first existence condition (4), and $\Delta_2(x,y)<0$ for any value of (x,y). Consequently, there are no periodic dynamics in the interior of the positive quadrants of the xz-plane and xy-plane.

Theorem 4. System (2) is uniformly persistent if the following conditions are met:

$$\mu_7<\mu_1, \tag{30}$$

$$\frac{\mu_2(1+\mu_3\tilde{z})\tilde{z}}{1+\mu_4}+\mu_7<\frac{\mu_1}{1+\tilde{z}}. \tag{31}$$

$$\mu_9\hat{y}+\mu_{12}<\frac{\mu_8(\hat{y}+\mu_{13})}{1+\mu_4+\mu_5\hat{y}^2}. \tag{32}$$

Proof. Define the function $\Phi(x,y,z)=x^{\rho_1}y^{\rho_2}z^{\rho_3}$, where ρ_1,ρ_2,ρ_3 are arbitrary positive constants, and $\Phi(x,y,z)>0$ for all $(x,y,z)\in\mathbb{R}^3_+$ with $\Phi(x,y,z)\to 0$ if either x,y or z goes to zero. Now, let

$$\Psi(x,y,z)=\frac{\Phi'(x,y,z)}{\Phi(x,y,z)}=\rho_1 f_1+\rho_2 f_2+\rho_3 f_3.$$

The functions $f_1, f_2,$ and f_3 are defined in system (2).

The average Lyapunov approach requires demonstrating that the function $\Psi(x,y,z)>0$ at all boundary equilibrium points [34]. Thus,

$$\begin{aligned}\Psi(x,y,z)=&\rho_1\left[1-x-\frac{y}{1+z}\right]+\rho_2\left[\frac{\mu_1 x}{1+z}-\frac{\mu_2(1+\mu_3 z)z}{1+\mu_4+\mu_5 y^2}-\mu_6 y^2-\mu_7\right]\\&+\rho_3\left[\frac{\mu_8(1+\mu_3 z)(y+\mu_{13})}{1+\mu_4+\mu_5 y^2}-\frac{\mu_9 y}{1+\mu_{10}z}-\mu_{11}z-\mu_{12}\right]\end{aligned}.$$

That implies

$$\Psi(e_0)=\rho_1[1]+\rho_2[-\mu_7]+\rho_3\left[\frac{\mu_8\mu_{13}}{1+\mu_4}-\mu_{12}\right].$$

Clearly, by allowing the arbitrary positive constant ρ_1 to be sufficiently greater than the positive constants ρ_2 and ρ_3, $\Psi(e_0)>0$ is obtained.

$$\Psi(e_1)=\rho_2[\mu_1-\mu_7]+\rho_3\left[\frac{\mu_8\mu_{13}}{1+\mu_4}-\mu_{12}\right].$$

According to condition (30), if the positive constant ρ_2 is sufficiently greater than the positive constant ρ_3, then $\Psi(e_1)>0$ is obtained.

$$\Psi(e_2)=\rho_1[1]+\rho_2\left[-\frac{\mu_2(1+\mu_3\tilde{z})\tilde{z}}{1+\mu_4}-\mu_7\right].$$

Hence, allowing the arbitrary positive constant ρ_1 to be sufficiently greater than the positive constants ρ_2, it obtained $\Psi(e_2)>0$.

$$\Psi(e_3) = \rho_2\left[\frac{\mu_1}{1+\tilde{z}} - \frac{\mu_2(1+\mu_3\tilde{z})\tilde{z}}{1+\mu_4} - \mu_7\right].$$

Hence, due to condition (31), it is obtained that $\Psi(e_3) > 0$. Finally, at this point e_4, direct calculation shows that:

$$\Psi(e_4) = \rho_3\left[\frac{\mu_8(\hat{y}+\mu_{13})}{1+\mu_4+\mu_5\hat{y}^2} - \mu_9\hat{y} - \mu_{12}\right].$$

It is obtained that $\Psi(e_3) > 0$ under condition (32). Thus, the system (2) is uniformly persistent, therefore the proof is done. ■

5. GLOBAL STABILITY ANALYSIS

In this part, appropriate Lyapunov functions are used to explore the global stability within the bounded region Ψ of the system's (2) locally asymptotically stable equilibrium points, as demonstrated in the following theorems.

Theorem 5. The first axial point e_1 of the system (2) is globally asymptotically stable whenever it is locally asymptotically stable.

Proof. Define the real-valued function $G_1(x,y,z) = (x - 1 - \ln x) + \frac{1}{\mu_1}y + \frac{\mu_2}{\mu_1\mu_8}z$, which is a positive definite function since $G_1(e_1) = 0$ and $G_1(x,y,z) > 0$ for all $\{(x,y,z) \in \mathbb{R}^3_+ : x > 0, y \geq 0, z \geq 0\}$, and $(x,y,z) \neq e_1$. Furthermore, some direct computation yields:

$$\frac{dG_1}{dt} \leq -(x-1)^2 - \left[\frac{\mu_7}{\mu_1} - 1\right]y - \frac{\mu_2}{\mu_1}\left[\frac{\mu_{11}}{\mu_8} - \frac{\mu_3\mu_{13}}{(1+\mu_4)}\right]z^2 - \frac{\mu_2}{\mu_1}\left[\frac{\mu_{12}}{\mu_8} - \frac{\mu_{13}}{(1+\mu_4)}\right]z.$$

Consequently, $\frac{dG_1}{dt}$ is a negatively definite function under the local stability conditions in the bounded region Ψ. Hence e_1 is globally asymptotically stable. ■

Theorem 6. If the first planar point e_3 is locally asymptotically stable, it is globally asymptotically stable, provided that the following condition is met.

$$\mu_1 + \frac{\mu_2\mu_9}{\mu_8}\tilde{z} < \mu_7. \tag{33}$$

Proof. Consider the following a real-valued function

$$G_2(x,y,z) = (x - 1 - \ln x) + \frac{1}{\mu_1}y + \frac{\mu_2}{\mu_1\mu_8}\left(z - \tilde{z} - \tilde{z}\ln\left(\frac{z}{\tilde{z}}\right)\right).$$

It is a positive definite function since $G_2(e_3) = 0$ and $G_2(x,y,z) > 0$, for all $\{(x,y,z) \in \mathbb{R}^3_+ : x > 0, y \geq 0, z > 0\}$, and $(x,y,z) \neq (1,0,\tilde{z})$. Furthermore, some direct computation yields:

$$\frac{dG_2}{dt} = -(x-1)^2 + \frac{y}{1+z} - \frac{\mu_6}{\mu_1}y^3 - \frac{\mu_7}{\mu_1}y - \frac{\mu_2}{\mu_1}\frac{(1+\mu_3 z)y\tilde{z}}{(1+\mu_4+\mu_5 y^2)} + \frac{\mu_2}{\mu_1}\frac{\mu_3\mu_{13}(z-\tilde{z})^2}{(1+\mu_4+\mu_5 y^2)}$$
$$-\frac{\mu_2}{\mu_1}\frac{\mu_{13}\mu_5(1+\mu_3\tilde{z})y^2 z}{(1+\mu_4+\mu_5 y^2)(1+\mu_4)} + \frac{\mu_2}{\mu_1}\frac{\mu_{13}\mu_5(1+\mu_3\tilde{z})y^2\tilde{z}}{(1+\mu_4+\mu_5 y^2)(1+\mu_4)}$$
$$-\frac{\mu_2}{\mu_1\mu_8}\frac{\mu_9 yz}{1+\mu_{10}z} + \frac{\mu_2}{\mu_1\mu_8}\frac{\mu_9 y\tilde{z}}{1+\mu_{10}z} - \frac{\mu_2\mu_{11}}{\mu_1\mu_8}(z-\tilde{z})^2.$$

Therefore, it is obtained that:

$$\frac{dG_2}{dt} \le -(x-1)^2 - \left[\frac{\mu_7\mu_8-\mu_1\mu_8-\mu_2\mu_9\tilde{z}}{\mu_1\mu_8}\right]y + \frac{\mu_2}{\mu_1}\frac{\mu_{13}\mu_5(1+\mu_3\tilde{z})\tilde{z}}{(1+\mu_4)^2}y^2$$
$$-\frac{\mu_2}{\mu_1}\left[\frac{\mu_{11}}{\mu_8} - \frac{\mu_3\mu_{13}}{(1+\mu_4)}\right](z-\tilde{z})^2.$$

Consequently, $\frac{dG_2}{dt}$ is a negatively definite function under the condition (33) along with the local stability condition and the logistic function form of y. Hence e_3 is globally asymptotically stable.

Theorem 7. The second planar point e_4 is globally asymptotically stable, provided the following conditions hold.

$$\frac{\mu_1\hat{y}}{\mu_2} + \frac{(\hat{y}+\mu_{13})}{(1+\mu_4)} < \frac{\mu_{12}}{\mu_8}. \quad (34)$$

$$\frac{\mu_3(\hat{y}+\mu_{13})}{(1+\mu_4)} < \frac{\mu_{11}}{\mu_8}. \quad (35)$$

Proof. Define $G_3(x,y,z) = \left(x - \hat{x} - \hat{x}\ln\frac{x}{\hat{x}}\right) + \frac{1}{\mu_1}\left(y - \hat{y} - \hat{y}\ln\frac{y}{\hat{y}}\right) + \frac{\mu_2}{\mu_1\mu_8}z$, which is real-valued function. It is a positive definite function since $G_3(e_4) = 0$ and $G_3(x,y,z) > 0$, for all $\{(x,y,z) \in \mathbb{R}^3_+ : x > 0, y > 0, z \ge 0\}$, and $(x,y,z) \ne (\hat{x},\hat{y},0)$. Furthermore, some direct computation yields:

$$\frac{dG_3}{dt} \le -(x-\hat{x})^2 - \frac{\mu_6}{\mu_1}(y+\hat{y})(y-\hat{y})^2 - \frac{\mu_2}{\mu_1}\left[\frac{\mu_{11}}{\mu_8} - \frac{\mu_3(\hat{y}+\mu_{13})}{(1+\mu_4)}\right]z^2$$
$$-\frac{\mu_2}{\mu_1}\left[\frac{\mu_{12}}{\mu_8} - \frac{\mu_1\hat{y}}{\mu_2} - \frac{(\hat{y}+\mu_{13})}{(1+\mu_4)}\right]z.$$

Consequently, $\frac{dG_3}{dt}$ is a negatively definite function under the conditions (34)-(35). Hence e_4 is globally asymptotically stable.

Theorem 8. The positive equilibrium point e_5 has a basin of attraction in the interior of Ψ that satisfies the following conditions.

$$\frac{\mu_2\mu_5\bar{z}(1+\mu_3\bar{z})}{(1+\mu_4)\bar{B}_2} < \mu_6, \quad (36)$$

$$\frac{\mu_8\mu_3(1+\mu_4)(\bar{y}+\mu_{13})}{(1+\mu_4)\bar{B}_2} + \frac{\mu_3\mu_5\mu_8\bar{y}^2(y_{max}+\mu_{13})}{(1+\mu_4)\bar{B}_2} + \frac{\mu_9\mu_{10}\bar{y}}{\bar{B}_3} < \mu_{11}, \quad (37)$$

$$M_{13}{}^2 < 2M_{33}, \quad (38)$$

$$M_{23}{}^{2} < 2M_{22}M_{33}, \tag{39}$$

where the new symbols are defined in the proof.

Proof. Consider the following real-valued function

$$G_4(x,y,z) = \left(x - \bar{x} - \bar{x}\ln\frac{x}{\bar{x}}\right) + \frac{1}{\mu_1}\left(y - \bar{y} - \bar{y}\ln\frac{y}{\bar{y}}\right) + \left(z - \bar{z} - \bar{z}\ln\frac{z}{\bar{z}}\right).$$

It is a positive definite function since $G_4(e_5) = 0$ and $G_4(x,y,z) > 0$, for all $\{(x,y,z) \in \mathbb{R}^3_+ : x > 0, y > 0, z > 0\}$, and $(x,y,z) \neq e_5$. Furthermore, some direct computation yields:

$$\begin{aligned}\frac{dG_4}{dt} &= -(x-\bar{x})^2 + \frac{\bar{y}}{B_1\bar{B}_1}(x-\bar{x})(z-\bar{z}) - \frac{1}{\mu_1}\left[\mu_6 - \frac{\mu_2\mu_5\bar{z}(1+\mu_3\bar{z})}{B_2\bar{B}_2}\right](y+\bar{y})(y-\bar{y})^2 \\ &\quad - \left[\mu_{11} - \frac{\mu_8\mu_3(1+\mu_4)(\bar{y}+\mu_{13})}{B_2\bar{B}_2} - \frac{\mu_3\mu_5\mu_8\bar{y}^2(y+\mu_{13})}{B_2\bar{B}_2} - \frac{\mu_9\mu_{10}\bar{y}}{B_3\bar{B}_3}\right](z-\bar{z})^2 \\ &\quad - \left[\frac{\bar{x}}{B_1\bar{B}_1} + \frac{\mu_2(1+\mu_3 z+\mu_3\bar{z})}{\mu_1 B_2} + \frac{\mu_8\mu_5\left(y\bar{y}+\mu_{13}(y+\bar{y})\right)(1+\mu_3\bar{z})}{B_2\bar{B}_2} + \frac{\mu_9}{B_3}\right. \\ &\quad \left. - \frac{\mu_8(1+\mu_4)(1+\mu_3 z)}{B_2\bar{B}_2}\right](y-\bar{y})(z-\bar{z}) = -(x-\bar{x})^2 + M_{13}(x-\bar{x})(z-\bar{z}) \\ &\quad - M_{22}(y-\bar{y})^2 - M_{33}(z-\bar{z})^2 - M_{23}(y-\bar{y})(z-\bar{z}),\end{aligned}$$

where $B_1 = (1+z), \bar{B}_1 = (1+\bar{z})$, $B_2 = (1+\mu_4+\mu_5 y^2), \bar{B}_2 = (1+\mu_4+\mu_5\bar{y}^2)$, $B_3 = (1+\mu_{10}z)$, and $\bar{B}_3 = (1+\mu_{10}\bar{z})$. While y_{max} is the upper bound of y within Ψ.

Therefore, according to the conditions (36)-(39) the derivative $\frac{dG_4}{dt}$ becomes negative definite. Hence, e_5 is an asymptotically stable point for any trajectory starting in the region that satisfies the given condition. Hence the proof is complete. ■

6. Local Bifurcation Analysis

This section employs the Sotomayor theorem [33] for local bifurcation to investigate how changing parameters impact the system's (2) qualitative dynamics close to non-hyperbolic points. Rewrite system (2) using the vector norm:

$$\frac{d\mathbf{X}}{dt} = \mathbf{F}(\mathbf{X},\mu), \mathbf{X} = (x,y,z)^T, \ \mathbf{F} = \left(xf_1(\mathbf{X},\mu), yf_2(\mathbf{X},\mu), zf_3(\mathbf{X},\mu)\right)^T,$$

where the system (2) specifies $f_i(\mathbf{X},\mu), \forall i = 1,2,3$. The potential bifurcation parameter $\mu \in \mathbb{R}$ is also specified. Direct computation of the second and third derivatives of vector $\mathbf{F}$ yields the following:

$$D^2\mathbf{F}(\mathbf{X},\mu).(\mathbf{V},\mathbf{V}) = (c_{i1})_{3\times 1}, \tag{40}$$

where $\mathbf{V} = (v_1, v_2, v_3)^T$ be any vector and

$$c_{11} = -2v_1^2 - \frac{2}{(1+z)}v_1v_2 + \frac{2y}{(1+z)^2}v_1v_3 + \frac{2x}{(1+z)^2}v_2v_3 - \frac{2xy}{(1+z)^3}v_3^2 \ ,$$

$$c_{21} = 2\frac{\mu_1(1+z)v_1v_2-\mu_1 y v_1 v_3}{(1+z)^2} - 2\left(\frac{\mu_1 x}{(1+z)^2} + \frac{\mu_2(1+2\mu_3 z)(1+\mu_4-\mu_5 y^2)}{(1+\mu_4+y^2\mu_5)^2}\right)v_2v_3$$
$$+2\left(\frac{\mu_1 x}{(1+z)^3} - \frac{\mu_2\mu_3}{1+\mu_4+\mu_5 y^2}\right)yv_3^2 + 2\left(\frac{z\mu_2\mu_5(1+\mu_3 z)(3+3\mu_4-\mu_5 y^2)}{(1+\mu_4+\mu_5 y^2)^3} - 3\mu_6\right)yv_2^2 .$$

$$c_{31} = 2\frac{\mu_5\mu_8[-3y(1+\mu_4)+\mu_5 y^3-\mu_{13}(1+\mu_4-3\mu_5 y^2)](1+\mu_3 z)z}{(1+\mu_4+\mu_5 y^2)^3}v_2^2$$
$$+2\left(\frac{\mu_9\mu_{10}y}{(1+\mu_{10}z)^3} - \mu_{11} + \frac{\mu_3\mu_8(y+\mu_{13})}{1+\mu_4+\mu_5 y^2}\right)v_3^2 .$$
$$+2\left(-\frac{\mu_9}{(1+\mu_{10}z)^2} + \frac{(1+2\mu_3 z)\mu_8(1+\mu_4-\mu_5 y(y+2\mu_{13}))}{(1+\mu_4+\mu_5 y^2)^2}\right)v_2v_3$$

Furthermore,

$$D^3\mathbf{F}(\mathbf{X},\mu).(\mathbf{V},\mathbf{V},\mathbf{V}) = (d_{i1})_{3\times 1}, \tag{41}$$

where:

$$d_{11} = \frac{6(1+z)^2}{(1+z)^4}v_1v_2v_3 - \frac{6x(1+z)}{(1+z)^4}v_2{v_3}^2 - \frac{6(1+z)y}{(1+z)^4}v_1{v_3}^2 + \frac{6xy}{(1+z)^4}{v_3}^3$$

$$d_{21} = -\frac{6\mu_1 xy}{(1+z)^4}v_3^3 - \frac{6\mu_1(1+z)}{(1+z)^3}v_1v_2v_3 + \frac{6\mu_1 y}{(1+z)^3}v_1{v_3}^2 + \frac{6\mu_2\mu_5 y(1+2\mu_3 z)(3+3\mu_4-\mu_5 y^2)}{(1+\mu_4+\mu_5 y^2)^3}v_2^2v_3$$
$$+\frac{6\mu_1 x}{(1+z)^3}v_2v_3^2 - 6\frac{\mu_2\mu_3(1+\mu_4-\mu_5 y^2)}{(1+\mu_4+\mu_5 y^2)^2}v_2v_3^2 .$$
$$+6v_2^3\left(\frac{z\mu_2(1+z\mu_3)\mu_5((1+\mu_4)^2-6y^2(1+\mu_4)\mu_5+y^4\mu_5^2)}{(1+\mu_4+y^2\mu_5)^4} - \mu_6\right)$$

$$d_{31} = -\frac{6y\mu_9\mu_{10}^2}{(1+z\mu_{10})^4}v_3^3 + \frac{6(1+2z\mu_3)\mu_5\mu_8(-3y(1+\mu_4)+y^3\mu_5-(1+\mu_4-3y^2\mu_5)\mu_{13})}{(1+\mu_4+y^2\mu_5)^3}v_2^2v_3$$
$$+6\left(\frac{\mu_9\mu_{10}}{(1+z\mu_{10})^3} + \frac{\mu_3\mu_8(1+\mu_4-y\mu_5(y+2\mu_{13}))}{(1+\mu_4+y^2\mu_5)^2}\right)v_2v_3^2 .$$
$$-\frac{6z(1+z\mu_3)\mu_5\mu_8[1+\mu_4^2+\mu_4(2-2y\mu_5(3y+2\mu_{13}))+y\mu_5(-6y-4\mu_{13}+y^2\mu_5(y+4\mu_{13}))]}{(1+\mu_4+y^2\mu_5)^4}v_2^3$$

Theorem 9: Near the first axial point, the system (2) experiences a transcritical bifurcation when the parameter μ_1 passes through the value $\mu_1^* = \mu_7$.

Proof: The matrix (13) at (e_1, μ_1^*) yields:

$$J_1 = J(e_1,\mu_1^*) = \begin{pmatrix} -1 & -1 & 0 \\ 0 & 0 & 0 \\ 0 & 0 & \frac{\mu_8\mu_{13}}{1+\mu_4} - \mu_{12} \end{pmatrix}.$$

The eigenvalues of J_1 are as follows: $\lambda_{11} = -1$, $\lambda_{12} = 0$, and $\lambda_{13} = \frac{\mu_8\mu_{13}}{1+\mu_4} - \mu_{12}$, which implies that e_1 non-hyperbolic point. Let $\mathrm{V}_1 = (v_{11}, v_{21}, v_{31})^T$, and $\mathrm{W}_1 = (w_{11}, w_{21}, w_{31})^T$ be the eigenvectors corresponding $\lambda_{12} = 0$ of J_1 and ${J_1}^T$ respectively. The straightforward computation yields that $\mathrm{V}_1 = (-1,1,0)^T$, $\mathrm{W}_1 = (0,1,0)^T$. Moreover, equation (40) is used to provide the following:

$$\mathbf{F}_{\mu_1} = \left(0, \frac{xy}{1+z}, 0\right)^T \Rightarrow \mathbf{F}_{\mu_1}(e_1,\mu_1^*) = (0,0,0)^T \Rightarrow \mathbf{W}_1^T\mathbf{F}_{\mu_1}(e_1,\mu_1^*) = 0.$$

$$\mathbf{W}_1^T\left[D\mathbf{F}_{\mu_1}(e_1,\mu_1^*).\mathbf{V}_1\right]=(0,1,0)\begin{pmatrix}0\\1\\0\end{pmatrix}=1\neq 0.$$

$$D^2\mathbf{F}(e_1,\mu_1^*).(\mathbf{V}_1,\mathbf{V}_1)=(0,-2\mu_1^*,0)^T \implies \mathbf{W}_1^T[D^2\mathbf{F}(e_1,\mu_1^*)(\mathbf{V}_1,\mathbf{V}_1)]=-2\mu_7\neq 0.$$

Hence, when $\mu_1^*=\mu_7$, system (2) experiences a transcritical bifurcation at the equilibrium point e_1. Thus, the proof is completed. ■

Theorem 10: Near the first planer point e_3, system (2) experiences a transcritical bifurcation when the parameter μ_7 passes through the positive value $\mu_7^*=\frac{\mu_1}{1+\tilde{z}}-\frac{\mu_2(1+\mu_3\tilde{z})\tilde{z}}{1+\mu_4}$ if the following condition holds:

$$2\frac{\mu_1}{(1+\tilde{z})}\theta_1-2\frac{\mu_1}{(1+\tilde{z})^2}\theta_2-2\frac{\mu_2(1+2\mu_3\tilde{z})}{(1+\mu_4)}\theta_2\neq 0, \tag{42}$$

where θ_1 and θ_2 are given in the proof. Otherwise, pitchfork bifurcation occurs when the following condition holds:

$$-\frac{6\mu_1}{(1+\tilde{z})^2}\theta_1\theta_2+\frac{6\mu_1}{(1+\tilde{z})^3}\theta_2^2-6\frac{\mu_2\mu_3}{(1+\mu_4)}\theta_2^2+6\left(\frac{\mu_2\mu_5(1+\mu_3\tilde{z})\tilde{z}}{(1+\mu_4)^2}-\mu_6\right)\neq 0. \tag{43}$$

Proof: The matrix (17) at (e_3,μ_7^*) yields:

$$J_2=J(e_3,\mu_7^*)=\begin{pmatrix}-1 & -\frac{1}{1+\tilde{z}} & 0\\ 0 & 0 & 0\\ 0 & \left(\frac{\mu_8(1+\mu_3\tilde{z})}{1+\mu_4}-\frac{\mu_9}{1+\mu_{10}\tilde{z}}\right)\tilde{z} & \left(\frac{\mu_3\mu_8\mu_{13}}{1+\mu_4}-\mu_{11}\right)\tilde{z}\end{pmatrix}.$$

The eigenvalues of J_2 are as follows: $\lambda_{31}=-1,\ \lambda_{32}=0$ and $\lambda_{33}=\left(\frac{\mu_3\mu_8\mu_{13}}{1+\mu_4}-\mu_{11}\right)\tilde{z}$. Hence a non-hyperbolic point e_3 has been obtained. Let $\mathbf{V}_2=(v_{12},v_{22},v_{32})^T$ and $\mathbf{W}_2=(w_{12},w_{22},w_{32})^T$ be the eigenvectors corresponding $\lambda_{32}=0$ of J_2 and ${J_2}^T$ respectively. The straightforward computation yields that $\mathbf{V}_2=(\theta_1,1,\theta_3)^T$, and $\mathbf{W}_2=(0,1,0)^T$, where $\theta_1=-\frac{1}{1+\tilde{z}}$ and $\theta_3=-\frac{\mu_8(1+\mu_3\tilde{z})(1+\mu_{10}\tilde{z})-\mu_9(1+\mu_4)}{(1+\mu_{10}\tilde{z})[\mu_3\mu_8\mu_{13}-\mu_{11}(1+\mu_4)]}$. Moreover, equation (40) is used to provide the following:

$$\mathbf{F}_{\mu_7}=(0,-y,0)^T \implies \mathbf{F}_{\mu_7}(e_3,\mu_7^*)=(0,0,0)^T \implies \mathbf{W}_2^T\mathbf{F}_{\mu_7}(e_3,\mu_7^*)=0.$$

$$\mathbf{W}_2^T\left[D\mathbf{F}_{\mu_7}(e_3,\mu_7^*).\mathbf{V}_2\right]=(0,1,0)\begin{pmatrix}0\\-1\\0\end{pmatrix}=-1\neq 0.$$

$$D^2\mathbf{F}(e_3,\mu_7^*).(\mathbf{V}_2,\mathbf{V}_2)=\begin{pmatrix}q_1\\q_2\\q_3\end{pmatrix}^T,$$

where:

$$q_1 = -2\theta_1^2 - \frac{2}{(1+\tilde{z})}\theta_1 + \frac{2}{(1+\tilde{z})^2}\theta_2 \;,$$

$$q_2 = 2\frac{\mu_1}{(1+\tilde{z})}\theta_1 - 2\frac{\mu_1}{(1+\tilde{z})^2}\theta_2 - 2\frac{\mu_2(1+2\mu_3\tilde{z})}{(1+\mu_4)}\theta_2.$$

$$q_3 = -2\frac{\mu_5\mu_8\mu_{13}(1+\mu_3\tilde{z})\tilde{z}}{(1+\mu_4)^2} + 2\left(-\mu_{11} + \frac{\mu_3\mu_8\mu_{13}}{1+\mu_4}\right)\theta_2^2 + 2\left(-\frac{\mu_9}{(1+\mu_{10}\tilde{z})^2} + \frac{(1+2\mu_3\tilde{z})\mu_8}{(1+\mu_4)}\right)\theta_2.$$

Thus

$$\mathbf{W}_2^T[D^2\mathbf{F}(e_3,\mu_7^*).(\mathbf{V}_2,\mathbf{V}_2)] = q_2.$$

Hence, when $\mu_7 = \mu_7^*$, the system (2) experiences a transcritical bifurcation at the equilibrium point e_3 when the condition (42) holds. However, when condition (42) fails to be met, equation (41) yields the following result:

$$D^3\mathbf{F}(e_3,\mu_7^*).(\mathbf{V}_2,\mathbf{V}_2,\mathbf{V}_2) = \begin{pmatrix} r_1 \\ r_2 \\ r_3 \end{pmatrix}^T,$$

where:

$$r_1 = \frac{6}{(1+\tilde{z})^2}\theta_1\theta_2 - \frac{6}{(1+\tilde{z})^3}\theta_2^2$$

$$r_2 = -\frac{6\mu_1}{(1+\tilde{z})^2}\theta_1\theta_2 + \frac{6\mu_1}{(1+\tilde{z})^3}\theta_2^2 - 6\frac{\mu_2\mu_3}{(1+\mu_4)}\theta_2^2 + 6\left(\frac{\mu_2\mu_5(1+\mu_3\tilde{z})\tilde{z}}{(1+\mu_4)^2} - \mu_6\right).$$

$$r_3 = -\frac{6(1+2\mu_3\tilde{z})\mu_5\mu_8\mu_{13}}{(1+\mu_4)^2}\theta_2 + 6\left(\frac{\mu_9\mu_{10}}{(1+\mu_{10}\tilde{z})^3} + \frac{\mu_3\mu_8}{(1+\mu_4)}\right)\theta_2^2 - \frac{6\mu_5\mu_8(1+\mu_3\tilde{z})\tilde{z}}{(1+\mu_4)^2}.$$

Hence

$$\mathbf{W}_2^T[D^3\mathbf{F}(e_3,\mu_7^*).(\mathbf{V}_2,\mathbf{V}_2,\mathbf{V}_2)] = r_2.$$

Thus, the proof proceeds and the pitchfork bifurcation occurs under the condition (43). ■

Theorem 11: Near the second planar equilibrium point, system (2) experiences a transcritical bifurcation when the parameter μ_{12} passes through the positive value $\mu_{12}^* = \frac{\mu_8(\hat{y}+\mu_{13})}{1+\mu_4+\mu_5\hat{y}^2} - \mu_9\hat{y}$ if the following condition holds:

$$-\frac{4\mu_5\mu_8\beta_2(\hat{y}+\mu_{13})\hat{y}}{(1+\mu_4+\mu_5\hat{y}^2)^2} + \frac{2\mu_8(\beta_2+\mu_3(y+\mu_{13}))}{1+\mu_4+\mu_5\hat{y}^2} - 2\mu_9(\beta_2 - \mu_{10}\hat{y}) - 2\mu_{11} \neq 0, \tag{44}$$

where β_2 is given in the proof. Otherwise, pitchfork bifurcation occurs when the following condition holds:

$$\frac{24\mu_8\mu_5^2\beta_2^2\hat{y}^3}{(1+\mu_4+\mu_5\hat{y}^2)^3} - \frac{6\mu_8\mu_5(3\beta_2\hat{y}+2\mu_3\hat{y}^2)\beta_2}{(1+\mu_4+\mu_5\hat{y}^2)^2} + \frac{6\mu_8\mu_3\beta_2}{1+\mu_4+\mu_5\hat{y}^2} + 6\mu_9\mu_{10}(\beta_2 - \mu_{10}\hat{y}) \neq 0. \tag{45}$$

Proof: The matrix (20) at (e_4,μ_{12}^*) yields:

$$J_3 = J(e_4, \mu_{12}^*) = \begin{pmatrix} -\hat{x} & -\hat{x} & \hat{x}\hat{y} \\ \mu_1\hat{y} & -2\mu_6\hat{y}^2 & -\mu_1\hat{x}\hat{y} - \frac{\mu_2\hat{y}}{1+\mu_4+\mu_5\hat{y}^2} \\ 0 & 0 & 0 \end{pmatrix}.$$

The eigenvalues of J_3 are as follows: $\lambda_{41,42} = -\mu_6\hat{y}^2 - \frac{\hat{x}}{2} \pm \frac{\sqrt{(2\mu_6\hat{y}^2+\hat{x})^2 - 4(2\mu_6\hat{x}\hat{y}^2+\mu_1\hat{x}\hat{y})}}{2}$, and $\lambda_{43} = 0$. This causes a non-hyperbolic point e_4 to be obtained. Let $\mathbf{V}_3 = (v_{13}, v_{23}, v_{33})^T$ and $\mathbf{W}_3 = (w_{13}, w_{23}, w_{33})^T$ be the eigenvectors corresponding $\lambda_{43} = 0$ of J_3 and $J_3{}^T$ respectively. The straightforward computation yields that $\mathbf{V}_3 = (\beta_1, \beta_2, 1)^T$, and $\mathbf{W}_3 = (0,0,1)^T$, where $\beta_1 = \hat{y} - \frac{\mu_1(\hat{y}-\hat{x})}{2\mu_6\hat{y}+\mu_1} + \frac{\mu_2}{(2\mu_6\hat{y}+\mu_1)(1+\mu_4+\mu_5\hat{y}^2)}$ and $\beta_2 = \frac{\mu_1(\hat{y}-\hat{x})}{2\mu_6\hat{y}+\mu_1} - \frac{\mu_2}{(2\mu_6\hat{y}+\mu_1)(1+\mu_4+\mu_5\hat{y}^2)}$. Moreover, equation (40) is used to provide the following:

$$\mathbf{F}_{\mu_{12}} = (0,0,-z)^T \implies \mathbf{F}_{\mu_{12}}(e_4, \mu_{12}^*) = (0,0,0)^T \implies \mathbf{W}_3^T \mathbf{F}_{\mu_{12}}(e_4, \mu_{12}^*) = 0.$$

$$\mathbf{W}_3^T\left[D\mathbf{F}_{\mu_{12}}(e_4, \mu_{12}^*).\mathbf{V}_3\right] = (0,0,1)\begin{pmatrix} 0 \\ 0 \\ -1 \end{pmatrix} = -1 \neq 0.$$

$$D^2\mathbf{F}(e_4, \mu_{12}^*).(\mathbf{V}_3, \mathbf{V}_3) = \begin{pmatrix} s_1 \\ s_2 \\ s_3 \end{pmatrix}^T,$$

where:

$$s_1 = -2\beta_1^2 - 2\beta_1\beta_2 + 2\beta_1\hat{y} + 2\beta_2\hat{x} - 2\hat{x}\hat{y} \;,$$

$$s_2 = 2\mu_1(\beta_1 - \hat{x})(\beta_2 - \hat{y}) + \frac{4\mu_2\mu_5\beta_2\hat{y}^2}{(1+\mu_4+\mu_5\hat{y}^2)^2} - \frac{2\mu_2(\beta_2+\mu_3\hat{y})}{1+\mu_4+\mu_5\hat{y}^2} - 6\mu_6\beta_2^2\hat{y},$$

$$s_3 = -\frac{4\mu_5\mu_8\beta_2(\hat{y}+\mu_{13})\hat{y}}{(1+\mu_4+\mu_5\hat{y}^2)^2} + \frac{2\mu_8\left(\beta_2+\mu_3(y+\mu_{13})\right)}{1+\mu_4+\mu_5\hat{y}^2} - 2\mu_9(\beta_2 - \mu_{10}\hat{y}) - 2\mu_{11}.$$

Thus

$$\mathbf{W}_3^T[D^2\mathbf{F}(e_4, \mu_{12}^*).(\mathbf{V}_3, \mathbf{V}_3)] = s_3.$$

Hence, when $\mu_{12} = \mu_{12}^*$, system (2) experiences a transcritical bifurcation at the equilibrium point e_4 if the condition (44) holds. When the condition (44) fails to be met, equation (41) yields the following result:

$$D^3\mathbf{F}(e_4, \mu_{12}^*).(\mathbf{V}_3, \mathbf{V}_3, \mathbf{V}_3) = \begin{pmatrix} u_1 \\ u_2 \\ u_3 \end{pmatrix}^T,$$

where:

$$u_1 = 6(\beta_1 - \hat{x})(\beta_2 - \hat{y}),$$

$$u_2 = -\frac{24\mu_2\mu_5^2\beta_2^2\hat{y}^3}{(1+\mu_4+\mu_5\hat{y}^2)^3} + \frac{6\mu_2\mu_5(3\mu_3\beta_2\hat{y}+2\mu_3\hat{y}^2)\beta_2}{(1+\mu_4+\mu_5\hat{y}^2)^2} - \frac{6\mu_2\mu_3\beta_2}{1+\mu_4+\mu_5\hat{y}^2},$$
$$-6\mu_1(\beta_1-\hat{x})(\beta_2-\hat{y}) - 6\mu_6\beta_2^3$$

$$u_3 = \frac{24\mu_8\mu_5^2\beta_2^2(\hat{y}+\mu_{13})\hat{y}^2}{(1+\mu_4+\mu_5\hat{y}^2)^3} - \frac{6\mu_5\mu_8((3\hat{y}+\mu_{13})\beta_2+2\mu_3(\hat{y}+\mu_{13})\hat{y})\beta_2}{(1+\mu_4+\mu_5\hat{y}^2)^2} + \frac{6\mu_8\mu_3\beta_2}{1+\mu_4+\mu_5\hat{y}^2}.$$
$$+6\mu_9\mu_{10}(\beta_2-\mu_{10}\hat{y})$$

Hence

$$\mathbf{W}_3^T[D^3\mathbf{F}(e_4,\mu_{12}^*).(\mathbf{V}_3,\mathbf{V}_3,\mathbf{V}_3)] = u_3.$$

Thus, the proof proceeds and the pitchfork bifurcation occur under the condition (45). ■

Theorem 12: Assuming the conditions (24)-(26) hold, as the parameter μ_{11} reaches the value $\mu_{11}^* = \frac{\mu_3\mu_8(\bar{y}+\mu_{13})}{1+\mu_4+\mu_5\bar{y}^2} + \frac{\mu_9\mu_{10}\bar{y}}{(1+\mu_{10}\bar{z})^2} - \frac{\bar{a}_{32}(\bar{a}_{11}\bar{a}_{23}-\bar{a}_{21}\bar{a}_{13})}{\bar{z}(\bar{a}_{11}\bar{a}_{22}-\bar{a}_{12}\bar{a}_{21})}$, system (2) experiences a saddle-node bifurcation around the positive point if the following condition holds:

$$w_{13}c_{11}^* + w_{23}c_{21}^* + c_{31}^* \neq 0, \tag{46}$$

where the definition of each new symbol is represented in the proof.

Proof: The matrix (22) at (e_5,μ_{11}^*) yields:

$$J_4 = J(e_5,\mu_{11}^*) = \begin{pmatrix} \bar{a}_{11} & \bar{a}_{12} & \bar{a}_{13} \\ \bar{a}_{21} & \bar{a}_{22} & \bar{a}_{23} \\ 0 & \bar{a}_{32} & \bar{a}_{33}^* \end{pmatrix},$$

where $\bar{a}_{33}^* = \bar{a}_{33}^*(\mu_{11}^*)$.

Simple computations show that the determinant of J_4, represented by α_3 in equation (23), is zero. Therefore, J_4 will have a zero eigenvalue ($\lambda_3^* = 0$) and two additional eigenvalues of negative real parts. Thus, the point e_5 becomes a non-hyperbolic point. Let $\mathbf{V}_4 = (v_{14},v_{24},v_{34})^T$ and $\mathbf{W}_4 = (w_{14},w_{24},w_{34})^T$ be the eigenvectors corresponding $\lambda_3^* = 0$ of J_4 and $J_4{}^T$ respectively. Then straightforward computation yields that:

$$\mathbf{V}_4 = \begin{pmatrix} \frac{\bar{a}_{12}\bar{a}_{23}-\bar{a}_{13}\bar{a}_{22}}{\bar{a}_{11}\bar{a}_{22}-\bar{a}_{12}\bar{a}_{21}} \\ -\frac{\bar{a}_{11}\bar{a}_{23}-\bar{a}_{13}\bar{a}_{21}}{\bar{a}_{11}\bar{a}_{22}-\bar{a}_{12}\bar{a}_{21}} \\ 1 \end{pmatrix} = \begin{pmatrix} v_{14} \\ v_{24} \\ 1 \end{pmatrix}, \quad \mathbf{W}_4 = \begin{pmatrix} \frac{\bar{a}_{21}\bar{a}_{32}}{\bar{a}_{11}\bar{a}_{22}-\bar{a}_{12}\bar{a}_{21}} \\ -\frac{\bar{a}_{11}\bar{a}_{32}}{\bar{a}_{11}\bar{a}_{22}-\bar{a}_{12}\bar{a}_{21}} \\ 1 \end{pmatrix} = \begin{pmatrix} w_{14} \\ w_{24} \\ 1 \end{pmatrix}.$$

Moreover, equation (40) is used to provide the following:

$$\mathbf{F}_{\mu_{11}} = (0,0,-z^2)^T \Rightarrow \mathbf{F}_{\mu_{11}}(e_5,\mu_{11}^*) = (0,0,-\bar{z}^2)^T$$
$$\Rightarrow \mathbf{W}_4^T\mathbf{F}_{\mu_{11}}(e_5,\mu_{11}^*) = \bar{z}^2 \neq 0 \,.$$

In addition, it is obtained that:

$$D^2\mathbf{F}(e_5,\mu_{11}^*).(\mathbf{V}_4,\mathbf{V}_4)=\begin{pmatrix}c_{11}^*\\c_{21}^*\\c_{31}^*\end{pmatrix}^T,$$

where $c_{11}^*=c_{11}(e_5,\mu_{11}^*,\mathbf{V}_4)$, $c_{21}^*=c_{21}(e_5,\mu_{11}^*,\mathbf{V}_4)$, and $c_{31}^*=c_{31}(e_5,\mu_{11}^*,\mathbf{V}_4)$. Hence, due to condition (46), it is obtained that:

$$\mathbf{W}_4^T[D^2\mathbf{F}(e_5,\mu_{11}^*).(\mathbf{V}_4,\mathbf{V}_4)]=w_{14}c_{11}^*+w_{24}c_{21}^*+c_{31}^*\neq 0$$

Hence, when $\mu_{11}=\mu_{11}^*$, system (2) experiences a Saddle-node bifurcation at the equilibrium point e_5. Thus, the proof is completed. ■

7. NUMERICAL SIMULATION

This section investigates many aspects of system (2) dynamics. The main objective is to learn how the system responds when its parameters are changed and verify the validity of the previously offered hypotheses and their results, by choosing biologically acceptable values for the parameters $\{\mu_i: 1\leq i\leq 13\}_{i\in\mathbb{N}}$. System (2) will be solved numerically, and the numerical solutions will be presented in different forms using MATLAB R2023b. The set S represents the set of parameters that are utilized to demonstrate the numerical trajectory shown in Fig. 1, using multiple initial points that are specified as $I_1=(0.75,0.75,0.75), I_2=(0.1,0.25,0.9), I_3=(0.9,0.1,0.9), I_4=(1,0.5,0.2)$, $I_5=(1,1,0.5), I_6=(0.5,0.25,0.75), I_7=(0.25,0.5,0.1), I_8=(0.5,0.5,0.5), I_9=(0.02,0.02,0.02)$ and $I_{10}=(0.2,0.01,0.01)$.

$$\begin{aligned}S=\{\mu_1=0.75,\mu_2=1.5,\mu_3=0.05,\mu_4=0.1,\mu_5=5,\mu_6=0.1,\mu_7=0.1,\\ \mu_8=0.8,\mu_9=0.1,\mu_{10}=5,\mu_{11}=0.1,\mu_{12}=0.1,\mu_{13}=0.1\}\end{aligned}\tag{47}$$

Note that, the red dots in the following phase portraits represent the approaching equilibrium points, while the blue dots refer to the starting points.

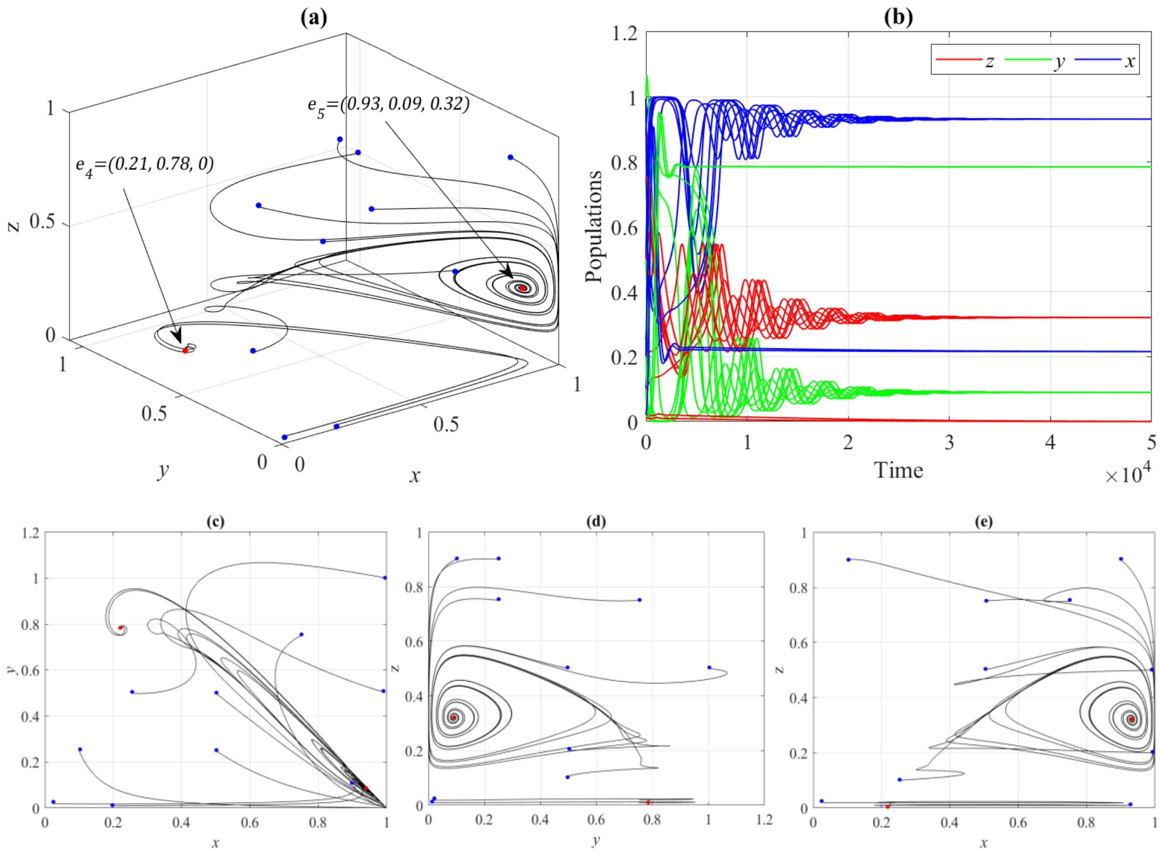

Figure 1. The trajectory of the system (2) using the set of parameters (47) shows a bi-stable behavior for system (2) between $e_4 = (0.21,0.78,0)$ and $e_5 = (0.93,0.09,0.32)$. (a) 3D phase portrait of the system (2) and its time series that is given in (b). (c) The projection of the phase portrait on the xy-plane. (d) The projection of the phase portrait on the yz-plane. (e) The projection of the phase portrait on the xz-plane.

According to Fig. 1, system (2) approaches to the positive point e_5 for the initial points $I_1, \dots, I_8$, and to the second planar point e_4 for the initial points I_9 and I_{10}, which suggests that the system exhibits bi-stable behavior. Moreover, the set of data (47) does not satisfy all the persistence conditions given in Theorem 4, and hence there is no guarantee for the persistence of the system.

Now, the changing of the parameter μ_1 and its effect on the system (2) appear to indicate that when $\mu_1 \leq 0.1$, the system approaches the first axial point e_1, the positive point e_5 will be the approaching point when $0.1 < \mu_1 < 0.66$ that indicates satisfying the persistence and global stability conditions, while the system (2) undergoes a bi-stable behavior between e_4 and e_5 for the range $0.66 \leq \mu_1 \leq 1.21$ as in Fig. 1. Moreover, when $\mu_1 > 1.21$ the system approaches e_4, see Fig. 2.

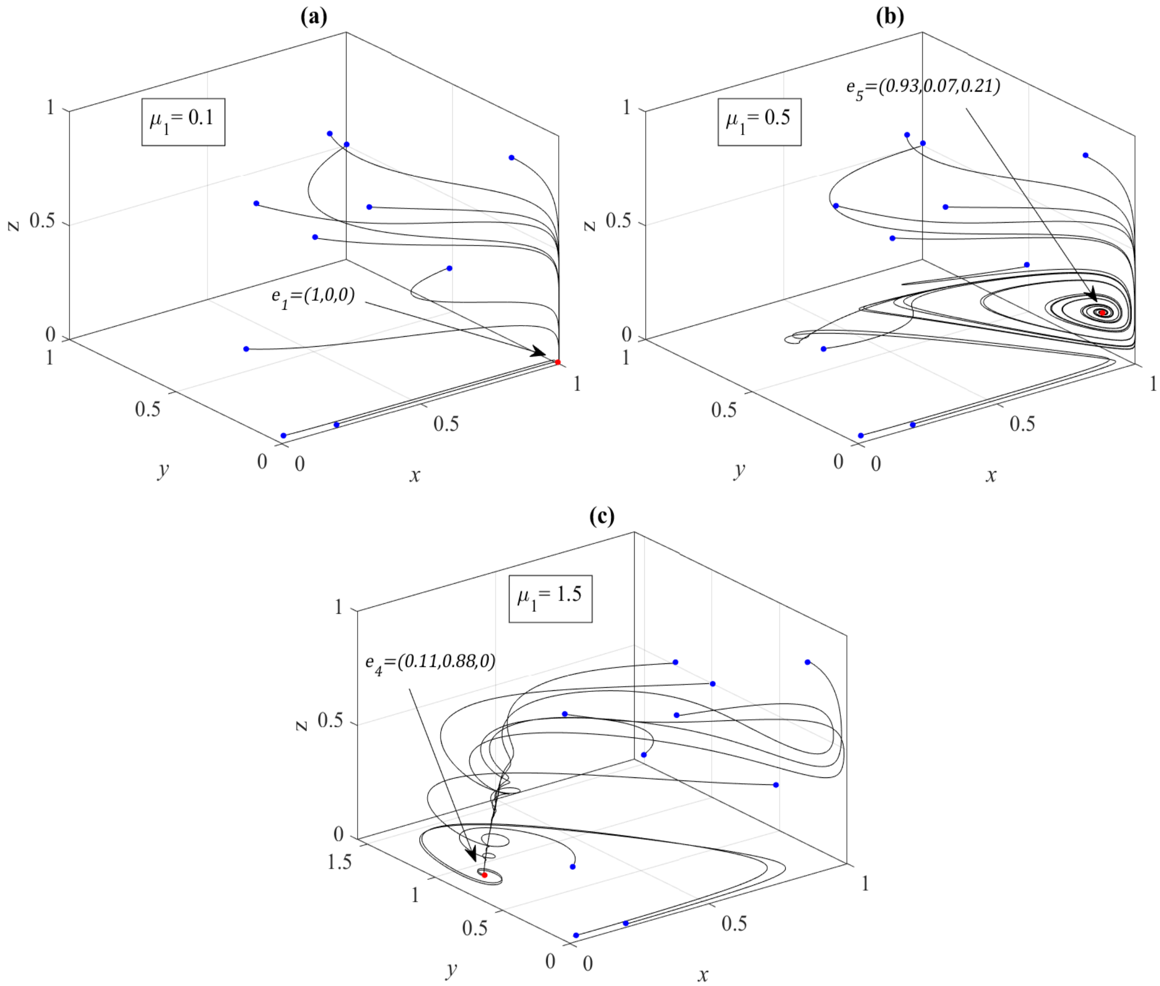

Figure 2. The bi-stable behavior of the system (2) with the set of parameters (47). (a) 3D phase portrait approaches $e_1 = (1,0,0)$ when $\mu_1 = 0.1$. (b) 3D phase portrait approaches $e_5 = (0.93,0.07,0.21)$ when $\mu_1 = 0.5$. (c) 3D phase portrait approaches $e_4 = (0.11,0.88,0)$ when $\mu_1 = 1.5$.

The effect of changing the parameter μ_2 on the dynamic behavior of the system (2) is only a quantitative impact so that the system still has a bi-stable behavior between the points e_4 and e_5 with an increase in the magnitude of the basin of attraction of the point e_4 for values in the range $\mu_2 > 4.7$, see Fig. 3.

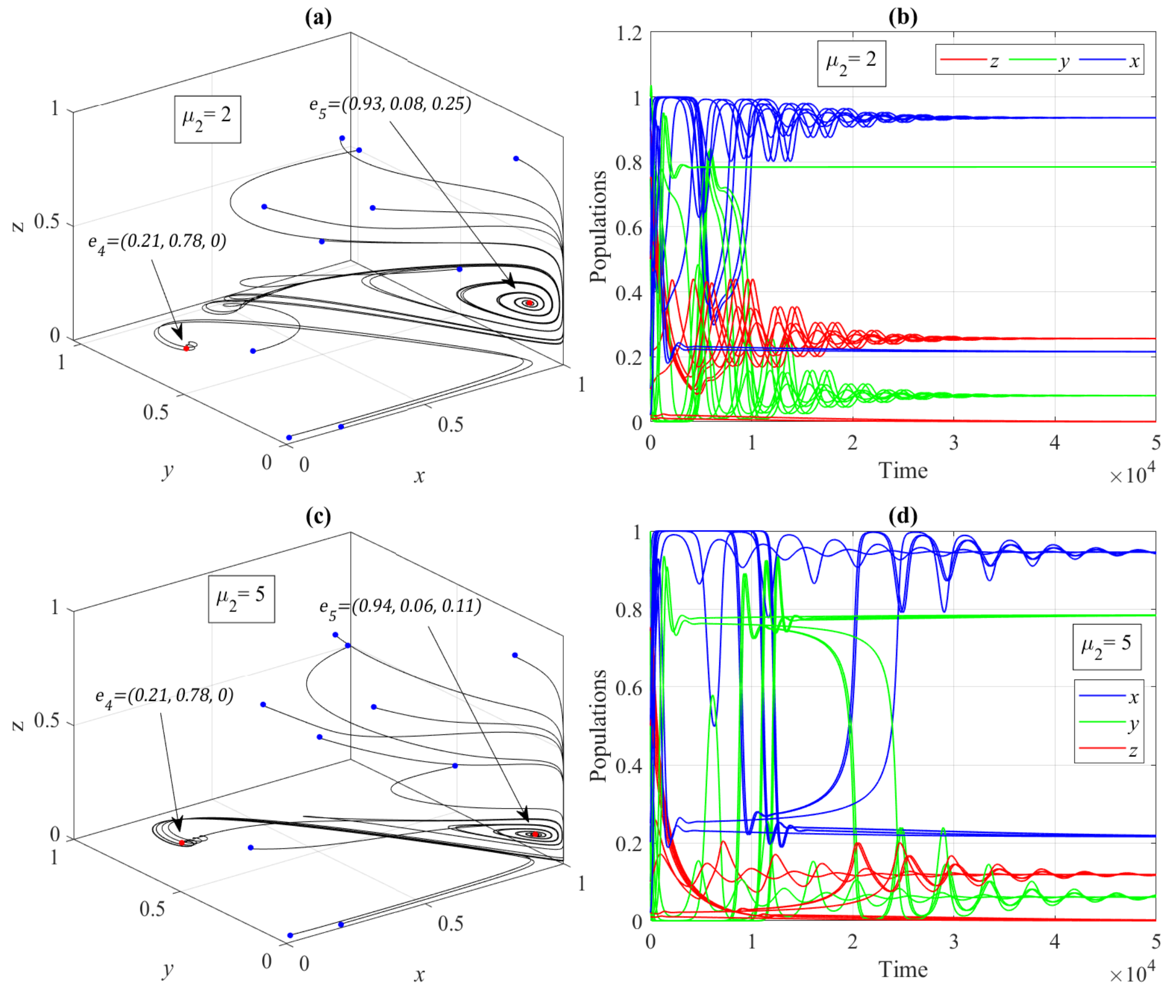

Figure 3. The bi-stable behavior of the system (2) with the set of parameters (47). (a) 3D phase portrait approaches $e_4 = (0.21,0.78,0)$ and $e_5 = (0.93,0.08,0.25)$ when $\mu_2 = 2$. (b) The time series with $\mu_2 = 2$. (c) 3D phase portrait approaches $e_4 = (0.21,0.78,0)$ and $e_5 = (0.94,0.06,0.11)$ when $\mu_2 = 5$. (d) The time series with $\mu_2 = 5$.

For the values of $\mu_3 < 1$, it is noted that the system (2) has a bi-stable behavior between e_4 and e_5, while it has a bi-stable behavior between e_4 and 3D periodic attractor for $1 < \mu_3 \leq 1.71$. However, system (2) has a bi-stable behavior between e_3 and e_4 when $\mu_3 > 1.71$, See Fig. 4.

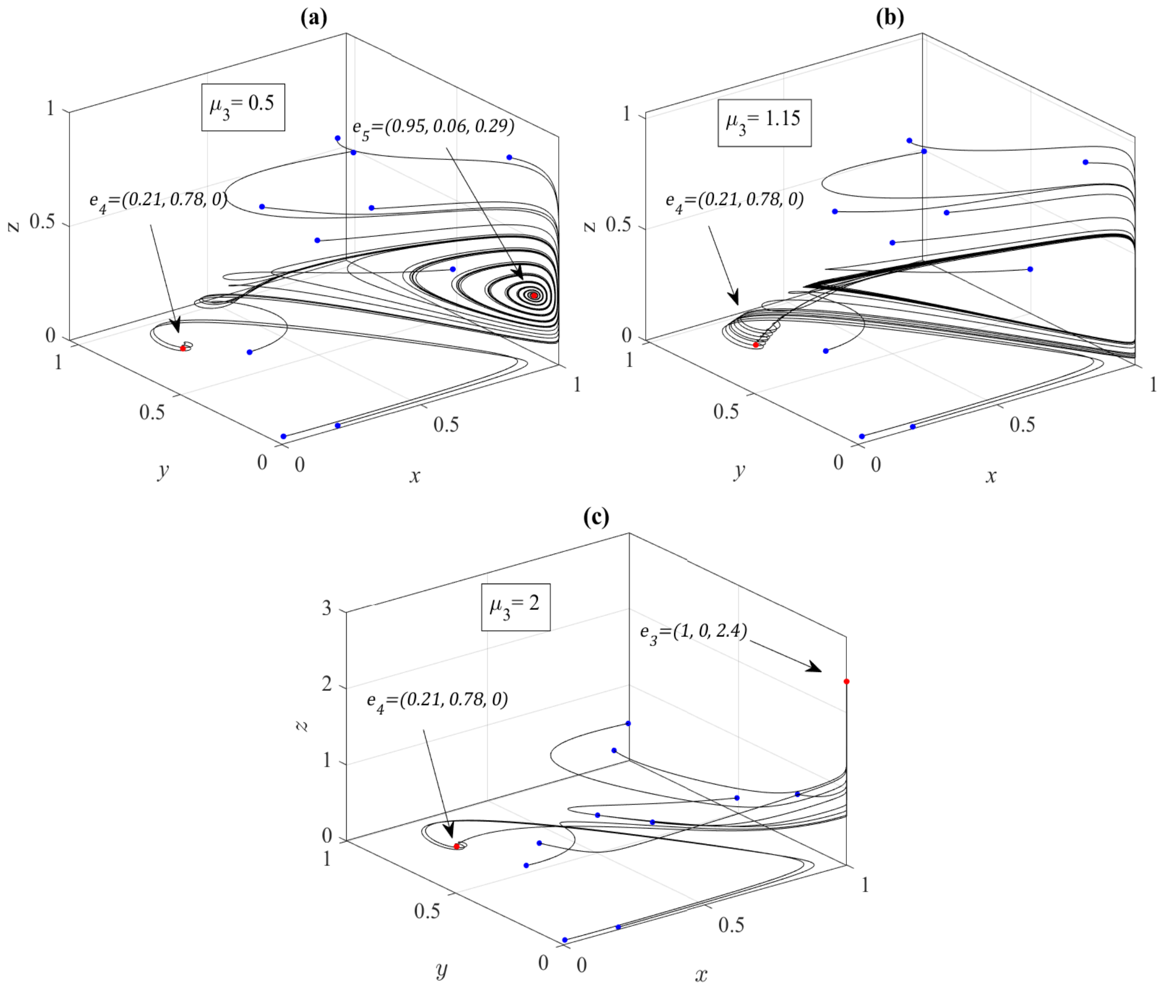

Figure 4. System (2) trajectories using the set of parameters (47). (a) 3D phase portrait shows bi-stable behavior between e_4 and e_5 when $\mu_3 = 0.5$. (b) 3D phase portrait shows bi-stable behavior between e_4 and 3D periodic attracter when $\mu_3 = 1.15$. (c) 3D phase portrait shows bi-stable behavior between $e_3 = (1,0,2.4)$ and e_4 when $\mu_3 = 2$.

Changing the parameter μ_6 and its effect on the system's (2) dynamic reveals that when $\mu_6 < 0.17$, the system has a bi-stable behavior between e_4 and e_5. However, for $\mu_6 \geq 0.17$, it approaches asymptotically from different initial points to the positive point e_5, it is observed all the conditions of persistence of the system are satisfied in this range. See Fig. 5.

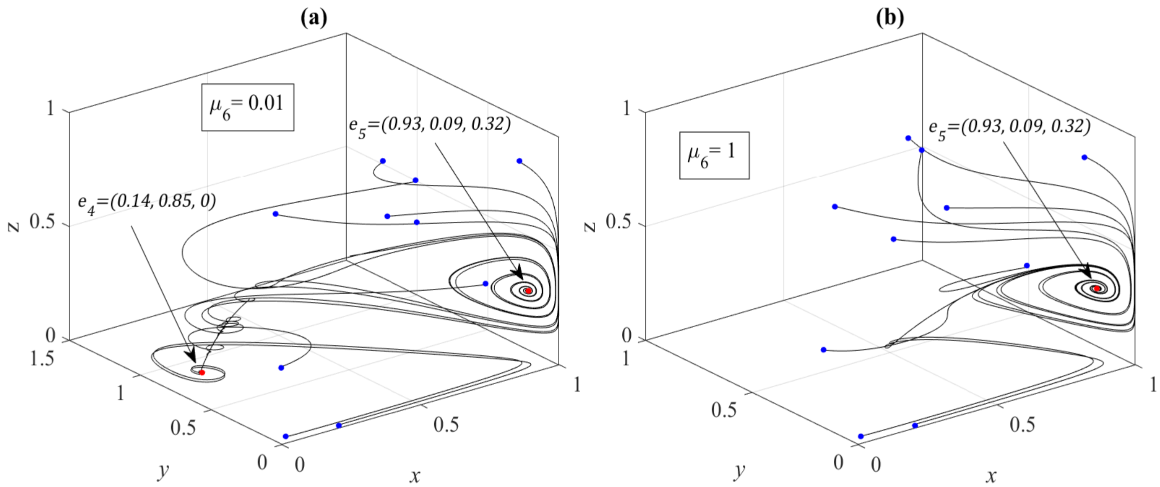

Figure 5. Using the data set (47) with different values of μ_6 shows that: (a) 3D phase portrait shows bi-stable behavior between $e_4 = (0.14,0.85,0)$ and $e_5 = (0.93,0.09,0.32)$ when $\mu_6 = 0.01$. (b) 3D phase portrait shows approaching $e_5 = (0.93,0.09,0.32)$ using different initial points when $\mu_6 = 1$.

The system's (2) dynamic is affected by varying the parameter μ_7, and the results indicate that when $\mu_7 < 0.14$ the system has a bi-stable behavior between e_4 and e_5. While, for the range $0.14 \leq \mu_7 < 0.75$ it approaches asymptotically the positive point e_5 starting from different initial points. Finally, when $\mu_7 \geq 0.75$, system (2) approaches asymptotically to the first axial point e_1. See Fig. 6.

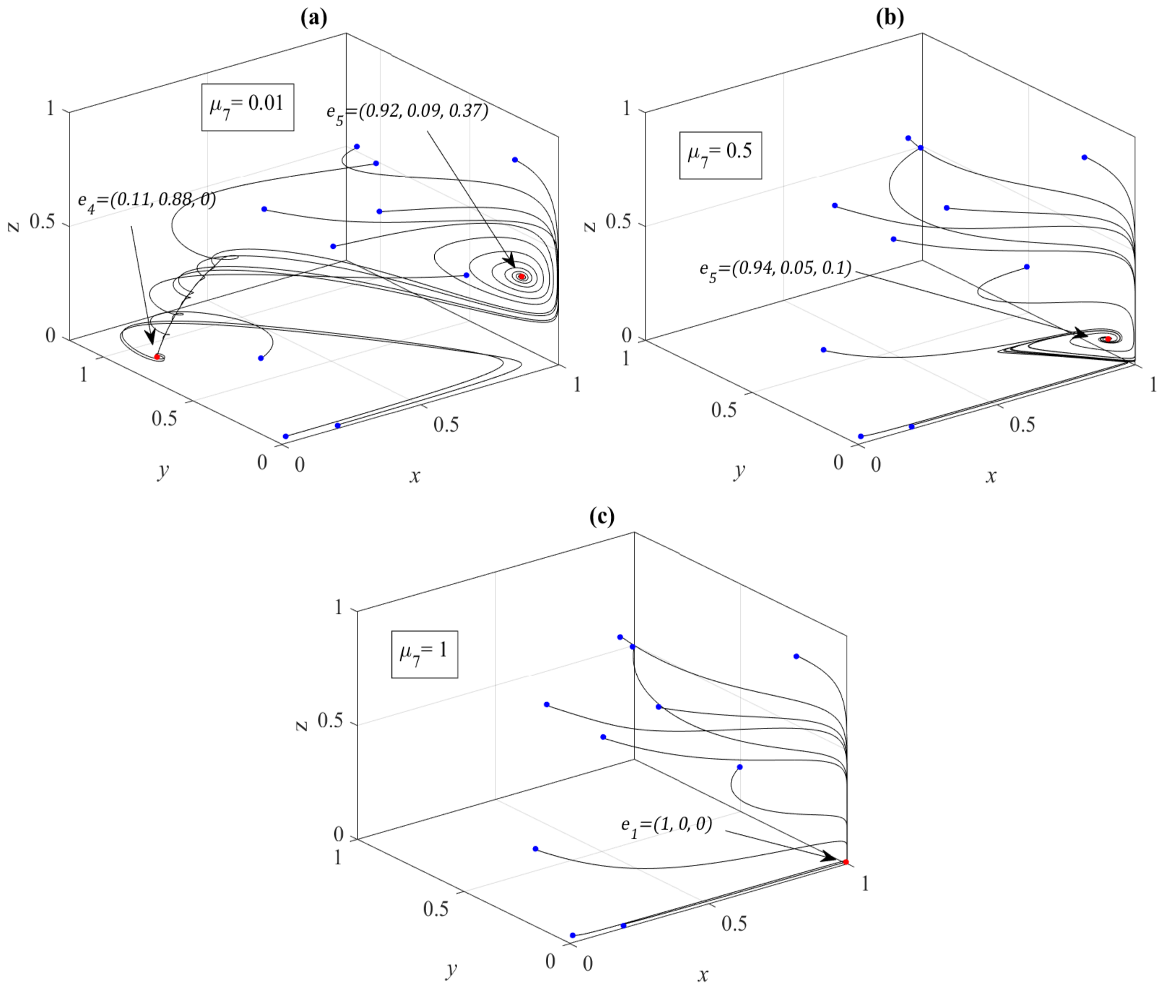

Figure 6. Using the data set (47) with different values of μ_7 shows that: (a) 3D phase portrait shows bi-stable behavior between $e_4 = (0.11,0.88,0)$ and $e_5 = (0.92,0.09,0.37)$ when $\mu_7 = 0.01$. (b) 3D phase portrait shows approaching $e_5 = (0.94,0.05,0.1)$ using different initial points when $\mu_7 = 0.5$. (c) 3D phase portrait shows approaching $e_1 = (1,0,0)$ using different initial points when $\mu_7 = 1$.

Now, adjusting the value of μ_8 affects the dynamics of the system (2). When $\mu_8 < 0.75$ the system approaches e_4. For $0.75 \leq \mu_8 < 0.85$ it has a bi-stable between e_4 and e_5 as shown in Fig. 1. For the range $0.85 \leq \mu_8 < 1.5$, the system approaches asymptotically the positive point e_5, it is observed all the conditions of persistence of the system (2) are satisfied in this range. Finally, when $\mu_8 \geq 1.5$, the system's persistence is lost due to the failure to achieve condition (30), and approaches asymptotically to the first planar point e_3. See Fig. 7.

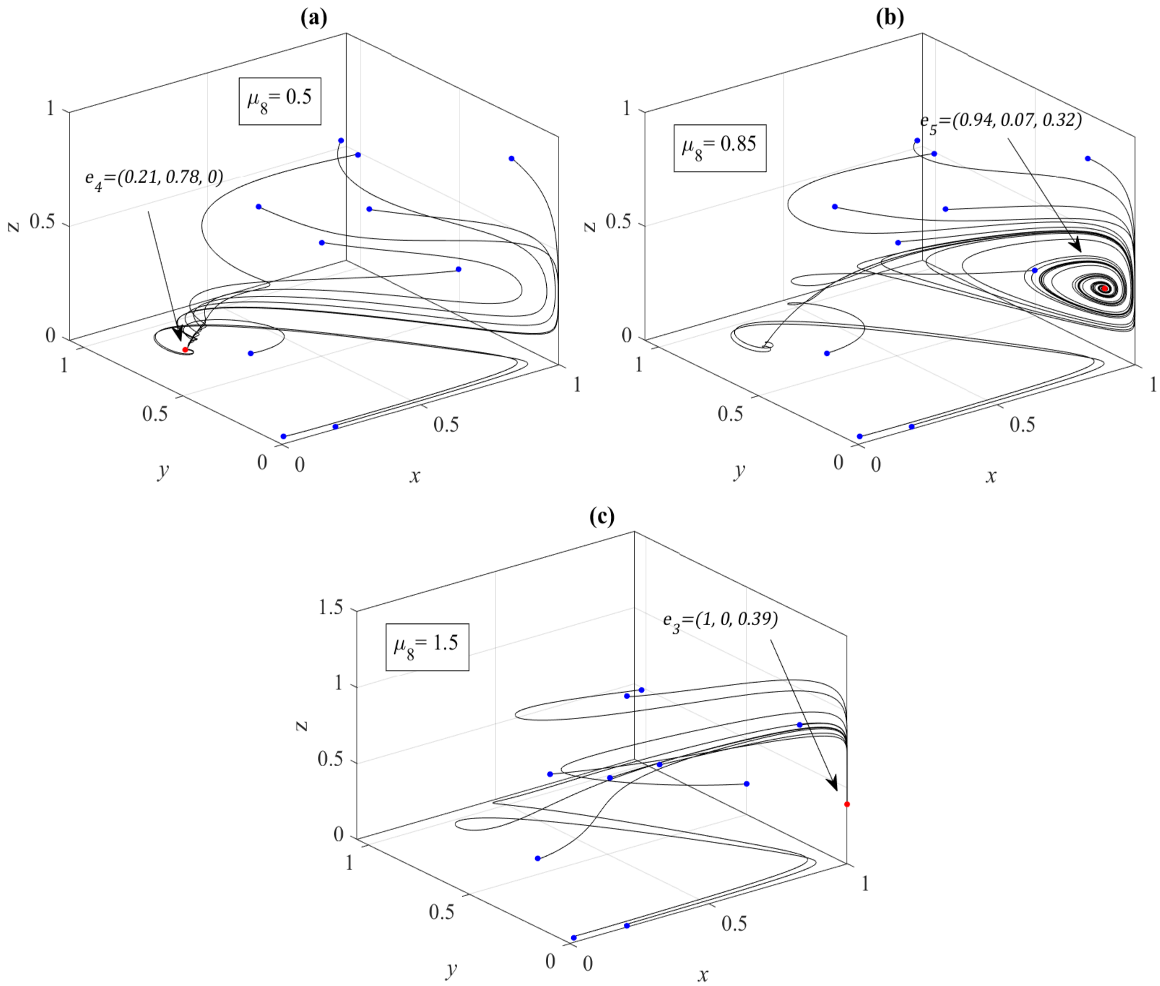

Figure 7. Using the data set (47) with different values of μ_8 shows that: (a) 3D phase portrait approaching $e_4 = (0.21,0.78,0)$ using different initial points when $\mu_8 = 0.5$. (b) 3D phase portrait approaching $e_5 = (0.94,0.07,0.32)$ when $\mu_8 = 0.85$. (c) 3D phase portrait approaching $e_3 = (1,0,0.39)$ when $\mu_8 = 1.5$.

It is observed from Fig. 7 that, increases in the value of μ_8 lead to reduce in the magnitude of the basin of attraction of e_4 and an increase in the magnitude of the basin of attraction of the point e_5 for the range $\mu_8 < 1.5$. However, for $\mu_8 > 1.5$, the system loses its persistence.

The effect of varying the parameter μ_{11} on the system's (2) dynamic shows that when $\mu_{11} \leq 0.01$, the system undergoes a bi-stable behavior between e_4 and a 3D periodic attracter. However, for the range $0.01 < \mu_{11} \leq 0.22$, the system (2) undergoes a bi-stable behavior between e_4 and e_5, as in Fig. 1. Moreover, the system approaches asymptotically to e_4 when $\mu_{11} > 0.22$, which means losing the persistence, see Fig. 8.

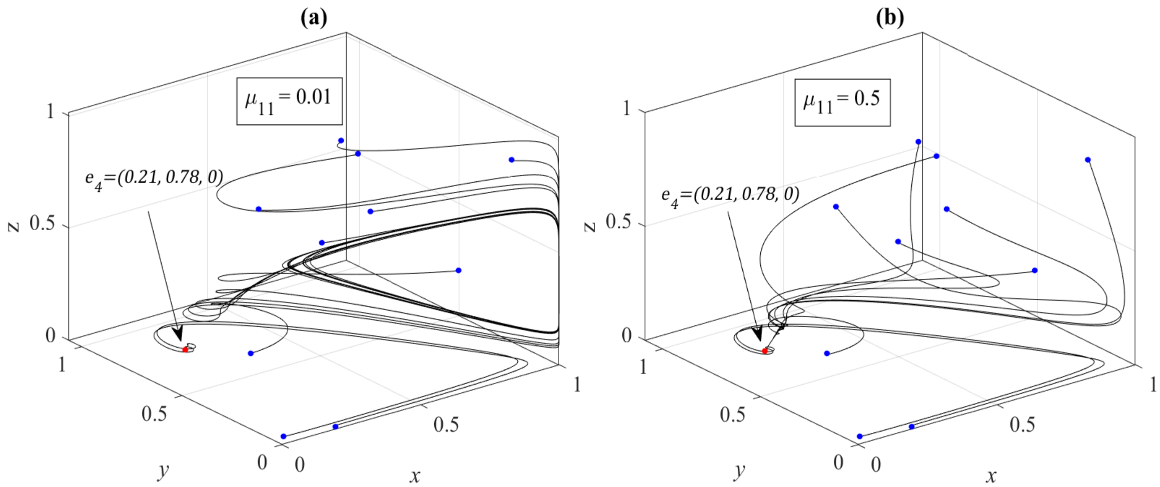

Figure 8. Using the data set (47) with different values of μ_{11} shows that: (a) 3D phase portrait shows bi-stable behavior between $e_4 = (0.21,0.78,0)$ and 3D periodic attracter when $\mu_{11} = 0.01$. (b) 3D phase portrait approaches e_4 when $\mu_{11} = 0.5$.

Now, the effect of changing the parameter μ_{12} on the system's (2) dynamic shows that when $\mu_{12} < 0.05$, the system approaches the first planar point e_3. In the range $0.05 \leq \mu_{12} \leq 0.09$, system (2) satisfies the persistence conditions and approaches asymptotically to the positive point e_5. Moreover, when $0.09 < \mu_{12} \leq 0.11$ the system (2) loses its persistence and the bi-stable behavior will take place as shown in Fig. 1. Furthermore, when $\mu_{12} > 0.11$ the system approaches the second planar point e_4 that means losing the persistence, see Fig. 9.

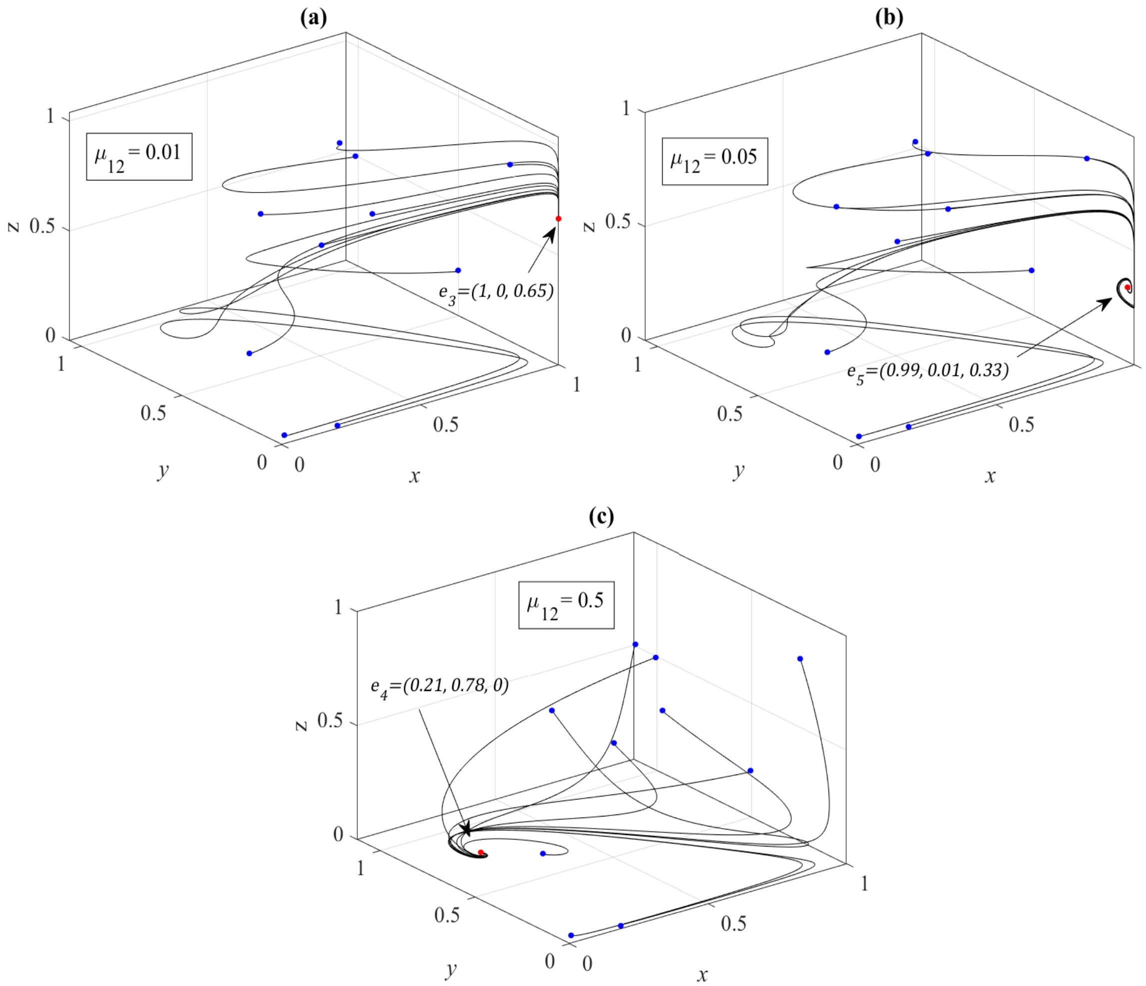

Figure 9. Using the data set (47) with different values of μ_{12} shows that: (a) 3D phase portrait approaches $e_3 = (1,0,0.65)$ when $\mu_{12} = 0.01$. (b) The phase portrait approaches $e_5 = (0.99,0.01,0.33)$ when $\mu_{12} = 0.05$. (c) 3D phase portrait approaches $e_4 = (0.21,0.78,0)$ when $\mu_{12} = 0.5$.

For the parameter μ_{13} in the range of $\mu_{13} \leq 0.03$ the system (2) has bi-stable behavior between the second planar point e_4 and the 3D periodic attracter. However, for the range $0.03 < \mu_{13} \leq 0.17$, the system approaches asymptotically to the positive point e_5 from different initial points. Furthermore, the system approaches e_3 when $0.17 < \mu_{13}$, see Fig. 10.

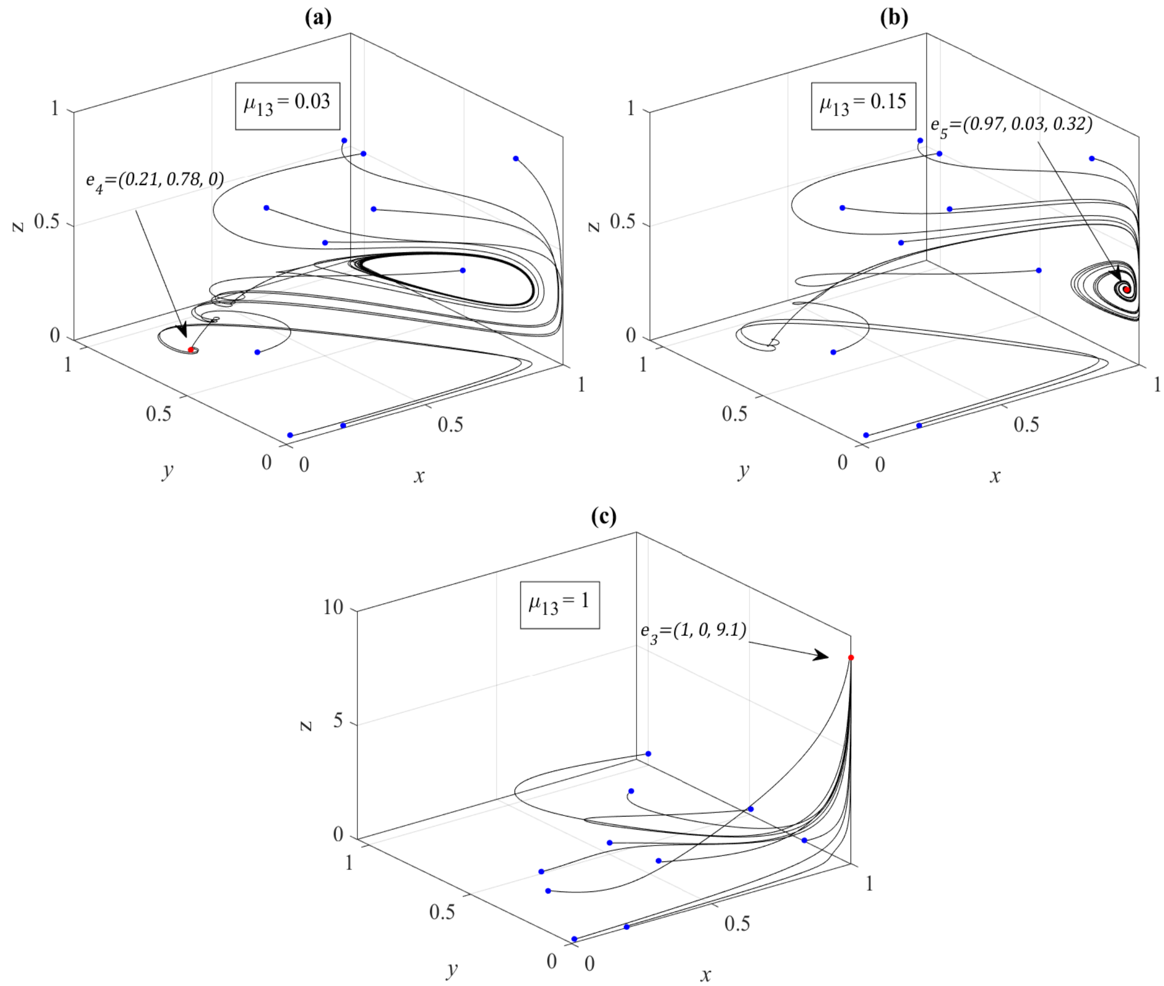

Figure 10. Using the data set (47) with different values of μ_{13} shows that: (a) 3D phase portrait explains bi-stable behavior between e_4 and 3D periodic attracter when $\mu_{13} = 0.03$. (b) 3D phase portrait approaches $e_5 = (0.97,0.03,0.32)$ when $\mu_{13} = 0.15$. (c) 3D phase portrait approaches $e_3 = (1,0,9.1)$ when $\mu_{13} = 1$.

Finally, it is observed that the impact of parameters μ_4, μ_5, and μ_9 on the system's (2) dynamic is similar to the impact of μ_2. It means that they have a quantitative effect on the system (2) dynamic so that the system (2) has a bi-stable behavior between points e_4 and e_5, with an increase in the magnitude of the basin of attraction of point e_4 and a decrease in the magnitude of the basin of attraction for e_5. On the other hand, although the parameter μ_{10} has a similar impact as that of μ_2 on the system's (2) dynamic, the magnitude of the basin of attraction of point e_5 increases, and the magnitude of the basin of attraction for e_4 decreases.

8. DISCUSSION AND CONCLUSIONS

An ecological food chain model including producer-consumer-predator was proposed. The influence of fear of predators, hunting cooperation, consumer's anti-predator capability, and availability of additional food for predators was investigated. The domain of the system's solution was specified. There are at most six equilibrium points, the origin, two axial points, two planar points, and the positive one. The linearization technique was used to investigate the local stability. Lyapunov functions were utilized to investigate the global dynamics. The average Lyapunov method was used to determine the persistence conditions. Local bifurcation analysis was carried out to specify the control set of parameters. Finally, numerical simulation was applied using an estimated set of biologically feasible parameters to confirm the analytical finding and understand the influence of varying the parameters. It is observed numerically that the system is rich in its dynamics including stable point, bi-stable between two equilibria, and bi-stable between equilibrium point and 3D periodic dynamics.

The parameter set is divided into different compartments regarding its impacts on the dynamic behavior of the proposed food chain. The stabilizing compartment contains the parameter $\mu_6 = \frac{q_1 r}{a_0^2}$, which is proportional to the stability at the positive equilibrium point and keeps the system persists. Accordingly, increasing the Toxicity coefficient for consumers or decreasing the consumer attack rate against producers has stabilizing impact on the system. The bi-stable compartment contains the parameters $\mu_2 = \frac{a_2}{rn}$, $\mu_3 = \frac{c}{na_2}$, $\mu_4 = \alpha\beta A$, $\mu_5 = \frac{m_0 r^2}{a_0^2}$, $\mu_9 = \frac{q_0}{a_0}$, and $\mu_{10} = \frac{m_1}{n}$, which has a quantitative impact of the dynamics of the system (2) but not qualitative, so that it does not satisfy the persistence conditions and does not affect them. Accordingly, the fear, additional food, hunting cooperation level, and the anti-predator coefficients have complicated and non-persistence impacts on the dynamic of the system. The extinction compartment contains the parameters $\mu_1 = \frac{a_1 k}{r}$, $\mu_7 = \frac{d_0}{r}$, $\mu_8 = \frac{ea_2}{a_0}$, $\mu_{11} = \frac{q_2}{nr}$, $\mu_{12} = \frac{d_1}{r}$, and $\mu_{13} = \frac{\beta A a_0}{r}$, which proportional to extinction in at least one of the consumer and predator. Therefore, the environment's carrying capacity, the natural death rates, the Toxicity coefficient for predators, and the effective additional food-level term have an extinction role in the food chain model.

CONFLICT OF INTERESTS

The author(s) declare that there is no conflict of interests.

REFERENCES

[1] É. Diz-Pita, M.V. Otero-Espinar, Predator–prey models: A review of some recent advances, Mathematics 9 (2021), 1783. https://doi.org/10.3390/math9151783.

[2] H.A. Satar, R.K. Naji, Stability and bifurcation in a prey–predator–scavenger system with Michaelis–Menten type of harvesting function, Differ. Equ. Dyn. Syst. 30 (2019), 933–956. https://doi.org/10.1007/s12591-018-00449-5.

[3] S.M.A. Al-Momen, R.K. Naji, The dynamics of modified Leslie-Gower predator-prey model under the influence of nonlinear harvesting and fear effect, Iraqi J. Sci. (2022), 259–282. https://doi.org/10.24996/ijs.2022.63.1.27.

[4] W. Sokol, J.A. Howell, Kinetics of phenol oxidation by washed cells, Biotech. Bioeng. 23 (1981), 2039–2049. https://doi.org/10.1002/bit.260230909.

[5] S. Al-Momen, R.K. Naji, The dynamics of Sokol-Howell prey-predator model involving strong Allee effect, Iraqi J. Sci. 62 (2021), 3114-3127. https://doi.org/10.24996/ijs.2021.62.9.27.

[6] F.H. Maghool, R.K. Naji, Chaos in the three-species Sokol-Howell food chain system with fear, Commun. Math. Biol. Neurosci. 2022 (2022), 14. https://doi.org/10.28919/cmbn/7056.

[7] K.P. Das, A study of harvesting in a predator-prey model with disease in both populations, Math. Methods Appl. Sci. 39 (2016), 2853-2870. https://doi.org/10.1002/mma.3735.

[8] D. Savitri, A. Suryanto, W.M. Kusumawinahyu, et al. Dynamical behavior of a modified Leslie–Gower one prey–two predators with competition, Mathematics. 8 (2020), 669. https://doi.org/10.3390/math8050669.

[9] M. Andersson, S. Erlinge, Influence of predation on rodent populations, Oikos 29 (1977) 591. https://doi.org/10.2307/3543597.

[10] M. Sen, P.D.N. Srinivasu, M. Banerjee, Global dynamics of an additional food provided predator-prey system with constant harvest in predators, Appl. Math. Comput. 250 (2015), 193-211. https://doi.org/10.1016/j.amc.2014.10.085.

[11] Q. Liu, D. Jiang, T. Hayat, et al. Stationary distribution and extinction of a stochastic predator–prey model with additional food and nonlinear perturbation, Appl. Math. Comput. 320 (2018), 226–239. https://doi.org/10.1016/j.amc.2017.09.030.

[12] S.M. Redpath, S.J. Thirgood, F.M. Leckie, Does supplementary feeding reduce predation of red grouse by hen harriers?, J. Appl. Ecol. 38 (2001), 1157–1168. https://doi.org/10.1046/j.0021-8901.2001.00683.x.

[13] M. Teixeira Alves, F.M. Hilker, Hunting cooperation and Allee effects in predators, J. Theor. Biol. 419 (2017), 13–22. https://doi.org/10.1016/j.jtbi.2017.02.002.

[14] X. Wang, L. Zanette, X. Zou, Modelling the fear effect in predator–prey interactions, J. Math. Biol. 73 (2016), 1179–1204. https://doi.org/10.1007/s00285-016-0989-1.

[15] A.R.M. Jamil, R.K. Naji, Modeling and analysis of the influence of fear on the harvested modified Leslie–Gower model involving nonlinear prey refuge, Mathematics 10 (2022), 2857. https://doi.org/10.3390/math10162857.

[16] P. Panday, N. Pal, S. Samanta, et al. Stability and bifurcation analysis of a three-species food chain model with fear, Int. J. Bifurcation Chaos 28 (2018), 1850009. https://doi.org/10.1142/s0218127418500098.

[17] M. Hossain, N. Pal, S. Samanta, Impact of fear on an eco-epidemiological model, Chaos, Solitons Fractals 134 (2020), 109718. https://doi.org/10.1016/j.chaos.2020.109718.

[18] N.H. Fakhry, R.K. Naji, The dynamics of a square root prey-predator model with fear, Iraqi J. Sci. 61 (2020), 139-146. https://doi.org/10.24996/ijs.2020.61.1.15.

[19] B. Tang, Y. Xiao, Bifurcation analysis of a predator–prey model with anti-predator behaviour, Chaos Solitons Fractals 70 (2015), 58–68. https://doi.org/10.1016/j.chaos.2014.11.008.

[20] X. Sun, Y. Li, Y. Xiao, A predator–prey model with prey population guided anti-predator behavior, Int. J. Bifurcation Chaos 27 (2017), 1750099. https://doi.org/10.1142/s0218127417500997.

[21] C. Li, Y. Zhang, J. Xu, et al. Global dynamics of a prey-predator model with antipredator behavior and two predators, Discr. Dyn. Nat. Soc. 2019 (2019), 3586508. https://doi.org/10.1155/2019/3586508.

[22] T.K. Ang, H.M. Safuan, J. Kavikumar, The impacts of harvesting activities on prey-predator fishery model in the presence of toxin, J. Sci. Technol. 10 (2018), 128-135. https://doi.org/10.30880/jst.2018.10.02.021.

[23] A.T. Keong, H.M. Safuan, K. Jacob, Dynamical behaviours of prey-predator fishery model with harvesting affected by toxic substances, Matematika (2018), 143–151. https://doi.org/10.11113/matematika.v34.n1.1018.

[24] Y. Louartassi, A. Alla, K. Hattaf, et al. Dynamics of a predator–prey model with harvesting and reserve area for prey in the presence of competition and toxicity, J. Appl. Math. Comput. 59 (2018), 305–321. https://doi.org/10.1007/s12190-018-1181-0.

[25] A. Das, G.P. Samanta, Modelling the fear effect in a two-species predator–prey system under the influence of toxic substances, Rend. Circ. Mat. Palermo, II. Ser 70 (2020), 1501–1526. https://doi.org/10.1007/s12215-020-00570-x.

[26] S.D. Zawka, P.D. Srinivasu, Optimal management of a prey-predator system in a polluted environment with effort shared between pollution reduction and harvesting, TWMS J. App. and Eng. Math. 14 (2024), 816-833.

[27] H.A. Satar, R.K. Naji, Stability and bifurcation of a prey-predator-scavenger model in the existence of toxicant and harvesting, Int. J. Math. Math. Sci. 2019 (2019), 1573516. https://doi.org/10.1155/2019/1573516.

[28] S.D. Zawka, T.T. Melese, Dynamics and optimal harvesting of prey-predator in a polluted environment in the presence of scavenger and pollution control, Math. Open. 2 (2023), 2350004. https://doi.org/10.1142/S2811007223500049.

[29] A.M. Sahi, H.A. Satar, The role of the fear, hunting cooperation, and anti-predator behavior in the prey-predator model having disease in predator, Commun. Math. Biol. Neurosci. 2024 (2024), 75. https://doi.org/10.28919/cmbn/8663.

[30] Z.M. Hadi, D.K. Bahlool, The effect of alternative resource and refuge on the dynamical behavior of food chain model, Malaysian J. Math. Sci. 17 (2023), 731-754. https://doi.org/10.47836/mjms.17.4.13.

[31] S.A. Rahi, R.K. Naji, The influence of fear, refuge, and additional food on the dynamics of a prey interacting with a predator having an infectious disease, Math. Model. Eng. Probl. 11 (2024), 1947-1960. https://doi.org/10.18280/mmep.110726.

[32] F. Chen, On a nonlinear nonautonomous predator–prey model with diffusion and distributed delay, J. Comput. Appl. Math. 180 (2005), 33-49. https://doi.org/10.1016/j.cam.2004.10.001.

[33] L. Perko, Differential equations and dynamical systems, 3rd edition, Springer, New York, 2001.

[34] V. Hutson, A theorem on average Liapunov functions, Monatsh. Math. 98 (1984), 267-275. https://doi.org/10.1007/bf01540776.